Progress In Electromagnetics Research, PIER 55, 1–31, 2005

HOMOGENIZATION OF CORRUGATED INTERFACES IN ELECTROMAGNETICS

G. Kristensson

Department of Electroscience
Lund Institute of Technology
P.O. Box 118, SE-221 00 Lund, Sweden

Abstract—A surface with periodic corrugations of sufficiently small periodicity is shown to be electromagnetically equivalent to an inhomogeneous transition region (slab). Explicit expressions for the inhomogeneous transition region are found for one-dimensional corrugations and for two-dimensional corrugations a local elliptic problem has to be solved in order to find the equivalent electromagnetic properties. The homogenized surface can be characterized by its surface impedance dyadic or its reflection dyadic. A few numerical examples illustrate the theory.

1. INTRODUCTION

This paper deals with the homogenization of the electromagnetic parameters of an interface between two dielectric materials where the interface shows a periodic variation on a length scale much smaller than the wavelength of the problem. The height of the periodic variation, however, needs not to be small compared to wavelength, but is arbitrary.

This problem in not new. Several attempts have been presented in the literature for the scalar problem [13], but less attention is paid to the electromagnetic case presumable due to its more complex structure. Approximative methods have been applied in the past, see *e.g.*, [3, 5, 6], but only few records of the exact limit result as the periodicity goes to zero seems to be reported in the literature.

The paper by Nevard and Keller [13] addresses both scalar and electromagnetic problems. The electromagnetic results reported in the paper by Nevard and Keller, however, are not correct. Specifically, the homogenization result for the electromagnetic problem in [13] shows an extra term in the homogenized Maxwell curl equations implying a coupling equivalent to that of a bianisotropic material. This form of the curl equations is also inconsistent with the corresponding divergence equations. This inconsistency was one of the reasons to revisit this homogenization problem, but also to exploit some of the potential applications of this problem and to develop its connection to the propagator technique to find the equivalent surface impedance of the homogenized material.

2. PREREQUISITES

The lateral position vector in the $\hat{\boldsymbol{e}}_1$-$\hat{\boldsymbol{e}}_2$-plane is denoted[†] $\boldsymbol{y} = \hat{\boldsymbol{e}}_1 y_1 + \hat{\boldsymbol{e}}_2 y_2$. The interface between the two homogeneous, isotropic materials is denoted $x_3 = h(\boldsymbol{y}) \in C^1_{\#}(Y)$ ($C^1_{\#}(Y)$ is the space of continuously differentiable functions in the unit cell $Y =]0, l_1[\times]0, l_2[$ that are Y-periodic), see Figure 1.

The permittivity $\epsilon(\boldsymbol{y}, x_3)$ is a Y-periodic function in the lateral variable $\boldsymbol{y}$, and defined by

$$\epsilon(\boldsymbol{y}, x_3) = \begin{cases} \epsilon_+, & x_3 > h(\boldsymbol{y}) \\ \epsilon_-, & x_3 < h(\boldsymbol{y}) \end{cases} \tag{1}$$

and similarly for the permeability $\mu(\boldsymbol{y}, x_3)$

$$\mu(\boldsymbol{y}, x_3) = \begin{cases} \mu_+, & x_3 > h(\boldsymbol{y}) \\ \mu_-, & x_3 < h(\boldsymbol{y}) \end{cases} \tag{2}$$

where $\epsilon^{\pm}$ and $\mu^{\pm}$ assume constant complex values. As a consequence, space consists of two different homogeneous, isotropic materials that have an interface with periodic corrugations in the lateral dimensions.

We denote the minimum and maximum values of $h(\boldsymbol{y})$ by h_- and h_+, respectively, see Figure 1, and the unit normal vector to the surface $\hat{\boldsymbol{\nu}}$, *i.e.*,

$$\hat{\boldsymbol{\nu}} = \frac{-\nabla_{\boldsymbol{y}} h(\boldsymbol{y}) + \hat{\boldsymbol{e}}_3}{\sqrt{1 + |\nabla_{\boldsymbol{y}} h(\boldsymbol{y})|^2}}$$

where gradient in the $\hat{\boldsymbol{e}}_1$-$\hat{\boldsymbol{e}}_2$-plane is denoted $\nabla_{\boldsymbol{y}} = \hat{\boldsymbol{e}}_1 \partial_1 + \hat{\boldsymbol{e}}_2 \partial_2$. This unit normal vector is assumed to be directed into the upper region[‡] with permittivity ϵ_+ and permeability μ_+, see Figure 1.

The intersection between the two different materials in the unit cell Y for fixed x_3 is defined by $x_3 = h(\boldsymbol{y})$ and denoted C, see Figure 1 c). We denote the two disjoint regions (not necessarily simply connected) separated by C by $Y_+(x_3)$ and $Y_-(x_3)$, respectively. The unit normal vector to C (lies in the $\hat{\boldsymbol{e}}_1$-$\hat{\boldsymbol{e}}_2$-plane) is

$$\hat{\boldsymbol{n}} = \frac{-\nabla_{\boldsymbol{y}} h(\boldsymbol{y})}{|\nabla_{\boldsymbol{y}} h(\boldsymbol{y})|}$$

[†] The local (microscopic) position variable is denoted $\boldsymbol{y}$ and the global (macroscopic) position vector $\boldsymbol{x}$ in this paper.

[‡] This expression of the unit normal vector assumes the $\nabla_{\boldsymbol{y}} h(\boldsymbol{y}) \neq \boldsymbol{0}$. Standard modifications have then to be made.

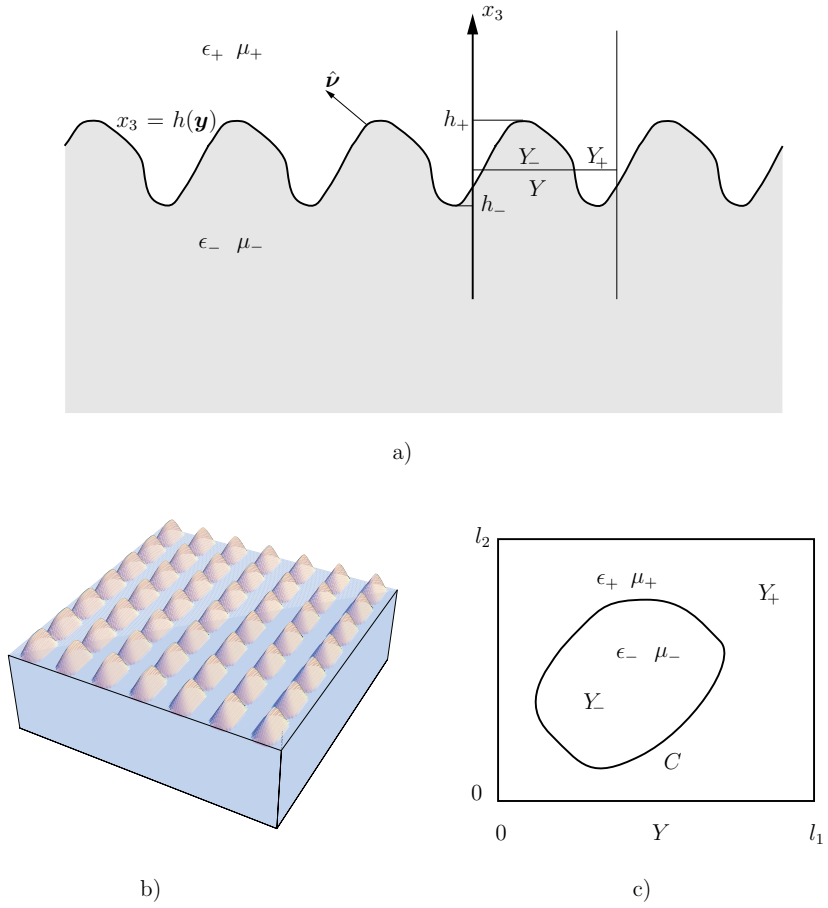

Figure 1. The interface problem and its geometry. a) The interface is given by the function $x_3 = h(\boldsymbol{y})$. The unit cell Y and its two disjoint parts $Y_\pm$ are shown. b) An interface with two-dimensional corrugations. c) The unit cell Y and its two disjoint parts $Y_\pm$ in the $\hat{\boldsymbol{e}}_1$-$\hat{\boldsymbol{e}}_2$-plane.

As a final remark, we notice that a slightly more general geometry with different permittivity or permeability outside the region $x_3 \in [h_-, h_+]$ can also be analyzed with the methods used in this paper. This leads to rather obvious and trivial extensions of the results and therefore not pursued here. However, the results are used in Section 6.

3. THE INTERFACE PROBLEM

We analyse the homogenization of a general two-dimensional corrugated surface in this section. The special properties of the homogenization of one-dimensional corrugations are presented in Section 4.

The underlying equations that model the behavior of the electromagnetic field on the microscale are the Maxwell equations.

$$\begin{cases} \nabla \times \boldsymbol{E}(\boldsymbol{x}) = \mathrm{i}k_0\mu \boldsymbol{H}(\boldsymbol{x}) \\ \nabla \times \boldsymbol{H}(\boldsymbol{x}) = -\mathrm{i}k_0\epsilon \boldsymbol{E}(\boldsymbol{x}) \end{cases}$$

which is assumed to hold in all space which is filled with the materials described in Section 2. The permittivity and permeability are given by (1) and (2), respectively. The wave number in vacuum is denoted $k_0 = \omega\sqrt{\epsilon_0\mu_0}$, where the permittivity and permeability of vacuum are denoted ϵ_0 and μ_0, respectively. These fields are subject to boundary conditions at the interface, $x_3 = h(\boldsymbol{y})$, between the two materials.

$$\begin{cases} [\hat{\boldsymbol{\nu}}(\boldsymbol{x}) \times \boldsymbol{E}(\boldsymbol{x})] = \boldsymbol{0} \\ [\hat{\boldsymbol{\nu}}(\boldsymbol{x}) \times \boldsymbol{H}(\boldsymbol{x})] = \boldsymbol{0} \\ [\hat{\boldsymbol{\nu}}(\boldsymbol{x}) \cdot \epsilon \boldsymbol{E}(\boldsymbol{x})] = 0 \\ [\hat{\boldsymbol{\nu}}(\boldsymbol{x}) \cdot \mu \boldsymbol{H}(\boldsymbol{x})] = 0 \end{cases} \tag{3}$$

where the bracket [ ] denotes the finite jump discontinuity at the boundary $x_3 = h(\boldsymbol{y})$, *i.e.*, the limit value of the field from above minus its limit value from below. We have here explicitly assumed that there is no surface current density present.

3.1. Multiple Scale Analysis—Basic Equations

We are now in a position to scale the problem and to investigate the limit of the solution to the Maxwell equations as the periodicity of the corrugations approaches zero. The permittivity and the permeability of the material are assumed to be Y^ε-periodic in the $\hat{\boldsymbol{e}}_1$-$\hat{\boldsymbol{e}}_2$-directions, *i.e.*,

$$\begin{cases} \epsilon((\boldsymbol{y} + \varepsilon l_i \hat{\boldsymbol{e}}_i)/\varepsilon, x_3) = \epsilon(\boldsymbol{y}/\varepsilon, x_3) \\ \mu((\boldsymbol{y} + \varepsilon l_i \hat{\boldsymbol{e}}_i)/\varepsilon, x_3) = \mu(\boldsymbol{y}/\varepsilon, x_3) \end{cases} \qquad i = 1, 2$$

where the Y-periodic permittivity and permeability are given by (1) and (2).

The solution to the Maxwell equations then satisfies

$$\left\{\begin{array}{l} \nabla\times\boldsymbol{E}^\varepsilon(\boldsymbol{x}) = \mathrm{i}k_0\mu(\boldsymbol{y}/\varepsilon,x_3)\boldsymbol{H}^\varepsilon(\boldsymbol{x}) \\ \nabla\times\boldsymbol{H}^\varepsilon(\boldsymbol{x}) = -\mathrm{i}k_0\epsilon(\boldsymbol{y}/\varepsilon,x_3)\boldsymbol{E}^\varepsilon(\boldsymbol{x}) \\ \nabla\cdot\{\epsilon(\boldsymbol{y}/\varepsilon,x_3)\boldsymbol{E}^\varepsilon(\boldsymbol{x})\} = 0 \\ \nabla\cdot\{\mu(\boldsymbol{y}/\varepsilon,x_3)\boldsymbol{H}^\varepsilon(\boldsymbol{x})\} = 0 \end{array}\right. \qquad \boldsymbol{x} = \boldsymbol{y} + \hat{\boldsymbol{e}}_3 x_3 \in \mathbb{R}^3$$

We adopt the method of multiple scales in this paper. This method is well established and found in may places in the literature [1, 12, 18], but for completeness some of the relevant steps in the derivation are presented. To this end, the solution is assumed to be of the form

$$\left\{\begin{array}{l} \boldsymbol{E}^\varepsilon(\boldsymbol{x}) = \boldsymbol{E}^{(0)}(\boldsymbol{x},\boldsymbol{y}) + \varepsilon\boldsymbol{E}^{(1)}(\boldsymbol{x},\boldsymbol{y}) + \ldots \\ \boldsymbol{H}^\varepsilon(\boldsymbol{x}) = \boldsymbol{H}^{(0)}(\boldsymbol{x},\boldsymbol{y}) + \varepsilon\boldsymbol{H}^{(1)}(\boldsymbol{x},\boldsymbol{y}) + \ldots \end{array}\right. \qquad \boldsymbol{x}\in\mathbb{R}^3, \boldsymbol{y}\in Y$$

The nabla operator takes the form $\nabla \to \nabla_{\boldsymbol{x}} + \varepsilon^{-1}\nabla_{\boldsymbol{y}}$, and the unit normal vector is proportional to $-\varepsilon^{-1}\nabla_{\boldsymbol{y}} h(\boldsymbol{y}) + \hat{\boldsymbol{e}}_3$.

Identification of powers of ε after these expansions have been introduced in the Maxwell equations implies ($j = -1, 0, 1, 2, \ldots$)

$$\left\{\begin{array}{l} \nabla_{\boldsymbol{x}}\times\boldsymbol{E}^{(j)}(\boldsymbol{x},\boldsymbol{y}) + \nabla_{\boldsymbol{y}}\times\boldsymbol{E}^{(j+1)}(\boldsymbol{x},\boldsymbol{y}) = \mathrm{i}k_0\mu(\boldsymbol{y},x_3)\boldsymbol{H}^{(j)}(\boldsymbol{x},\boldsymbol{y}) \\ \nabla_{\boldsymbol{x}}\times\boldsymbol{H}^{(j)}(\boldsymbol{x},\boldsymbol{y}) + \nabla_{\boldsymbol{y}}\times\boldsymbol{H}^{(j+1)}(\boldsymbol{x},\boldsymbol{y}) = -\mathrm{i}k_0\epsilon(\boldsymbol{y},x_3)\boldsymbol{E}^{(j)}(\boldsymbol{x},\boldsymbol{y}) \\ \nabla_{\boldsymbol{x}}\cdot\Big\{\epsilon(\boldsymbol{y},x_3)\boldsymbol{E}^{(j)}(\boldsymbol{x},\boldsymbol{y})\Big\} + \nabla_{\boldsymbol{y}}\cdot\Big\{\epsilon(\boldsymbol{y},x_3)\boldsymbol{E}^{(j+1)}(\boldsymbol{x},\boldsymbol{y})\Big\} = 0 \\ \nabla_{\boldsymbol{x}}\cdot\Big\{\mu(\boldsymbol{y},x_3)\boldsymbol{H}^{(j)}(\boldsymbol{x},\boldsymbol{y})\Big\} + \nabla_{\boldsymbol{y}}\cdot\Big\{\mu(\boldsymbol{y},x_3)\boldsymbol{H}^{(j+1)}(\boldsymbol{x},\boldsymbol{y})\Big\} = 0 \end{array}\right. \tag{4}$$

The boundary conditions in (3) imply ($j = -1, 0, 1, 2, \ldots$)

$$\left\{\begin{array}{l} \Big[\nabla_{\boldsymbol{y}} h(\boldsymbol{y})\times\boldsymbol{E}^{(j+1)}(\boldsymbol{x},\boldsymbol{y}) - \hat{\boldsymbol{e}}_3\times\boldsymbol{E}_t^{(j)}(\boldsymbol{x},\boldsymbol{y})\Big] = \boldsymbol{0} \\ \Big[\nabla_{\boldsymbol{y}} h(\boldsymbol{y})\times\boldsymbol{H}^{(j+1)}(\boldsymbol{x},\boldsymbol{y}) - \hat{\boldsymbol{e}}_3\times\boldsymbol{H}_t^{(j)}(\boldsymbol{x},\boldsymbol{y})\Big] = \boldsymbol{0} \\ \Big[\epsilon(\boldsymbol{y},x_3)\Big(\nabla_{\boldsymbol{y}} h(\boldsymbol{y})\cdot\boldsymbol{E}_t^{(j+1)}(\boldsymbol{x},\boldsymbol{y}) - E_3^{(j)}(\boldsymbol{x},\boldsymbol{y})\Big)\Big] = 0 \\ \Big[\mu(\boldsymbol{y},x_3)\Big(\nabla_{\boldsymbol{y}} h(\boldsymbol{y})\cdot\boldsymbol{H}_t^{(j+1)}(\boldsymbol{x},\boldsymbol{y}) - H_3^{(j)}(\boldsymbol{x},\boldsymbol{y})\Big)\Big] = 0 \end{array}\right. \qquad x_3 = h(\boldsymbol{y}) \tag{5}$$

where the bracket [ ] denotes the jump discontinuity at the boundary, and subscript t denotes the lateral (transverse) components of the fields. The vertical component of the fields is denoted by index 3.

3.2. First Order Term, $j = -1$

The lowest order term in equation (4) above is $j = -1$, *i.e.*,

$$\begin{cases} \nabla_{\boldsymbol{y}} \times \boldsymbol{E}^{(0)}(\boldsymbol{x},\boldsymbol{y}) = \nabla_{\boldsymbol{y}} \times \boldsymbol{E}_t^{(0)}(\boldsymbol{x},\boldsymbol{y}) + \nabla_{\boldsymbol{y}} E_3^{(0)}(\boldsymbol{x},\boldsymbol{y}) \times \hat{\boldsymbol{e}}_3 = \boldsymbol{0} \\ \nabla_{\boldsymbol{y}} \times \boldsymbol{H}^{(0)}(\boldsymbol{x},\boldsymbol{y}) = \nabla_{\boldsymbol{y}} \times \boldsymbol{H}_t^{(0)}(\boldsymbol{x},\boldsymbol{y}) + \nabla_{\boldsymbol{y}} H_3^{(0)}(\boldsymbol{x},\boldsymbol{y}) \times \hat{\boldsymbol{e}}_3 = \boldsymbol{0} \\ \nabla_{\boldsymbol{y}} \cdot \left\{ \epsilon(\boldsymbol{y},x_3) \boldsymbol{E}_t^{(0)}(\boldsymbol{x},\boldsymbol{y}) \right\} = 0 \\ \nabla_{\boldsymbol{y}} \cdot \left\{ \mu(\boldsymbol{y},x_3) \boldsymbol{H}_t^{(0)}(\boldsymbol{x},\boldsymbol{y}) \right\} = 0 \end{cases} \tag{6}$$

subject to the boundary conditions at $x_3 = h(\boldsymbol{y})$, see (5)

$$\begin{cases} \left[\nabla_{\boldsymbol{y}} h(\boldsymbol{y}) \times \boldsymbol{E}^{(0)}(\boldsymbol{x},\boldsymbol{y}) \right] = \boldsymbol{0} \\ \left[\nabla_{\boldsymbol{y}} h(\boldsymbol{y}) \times \boldsymbol{H}^{(0)}(\boldsymbol{x},\boldsymbol{y}) \right] = \boldsymbol{0} \end{cases}, \quad \begin{cases} \left[\epsilon(\boldsymbol{y},x_3) \nabla_{\boldsymbol{y}} h(\boldsymbol{y}) \cdot \boldsymbol{E}_t^{(0)}(\boldsymbol{x},\boldsymbol{y}) \right] = 0 \\ \left[\mu(\boldsymbol{y},x_3) \nabla_{\boldsymbol{y}} h(\boldsymbol{y}) \cdot \boldsymbol{H}_t^{(0)}(\boldsymbol{x},\boldsymbol{y}) \right] = 0 \end{cases}$$

which implies

$$\begin{cases} \left[\hat{\boldsymbol{n}} \times \boldsymbol{E}_t^{(0)}(\boldsymbol{x},\boldsymbol{y}) \right] = \boldsymbol{0} \\ \left[\hat{\boldsymbol{n}} \times \boldsymbol{H}_t^{(0)}(\boldsymbol{x},\boldsymbol{y}) \right] = \boldsymbol{0} \end{cases}, \quad \begin{cases} \left[E_3^{(0)}(\boldsymbol{x},\boldsymbol{y}) \right] = 0 \\ \left[H_3^{(0)}(\boldsymbol{x},\boldsymbol{y}) \right] = 0 \end{cases} \qquad x_3 = h(\boldsymbol{y})$$

The two curl equations in (6) imply that the third components of the electric and the magnetic fields are independent of $\boldsymbol{y}$, and, moreover, have the form

$$\begin{cases} \boldsymbol{E}^{(0)}(\boldsymbol{x},\boldsymbol{y}) = \nabla_{\boldsymbol{y}} \Phi(\boldsymbol{x},\boldsymbol{y}) + \boldsymbol{E}(\boldsymbol{x}) \\ \boldsymbol{H}^{(0)}(\boldsymbol{x},\boldsymbol{y}) = \nabla_{\boldsymbol{y}} \Psi(\boldsymbol{x},\boldsymbol{y}) + \boldsymbol{H}(\boldsymbol{x}) \end{cases}$$

where $\boldsymbol{E}(\boldsymbol{x})$ and $\boldsymbol{H}(\boldsymbol{x})$ are the average electric and magnetic fields, respectively, over the unit cell Y.

$$\begin{cases} \boldsymbol{E}(\boldsymbol{x}) = \dfrac{1}{|Y|} \iint\limits_Y \boldsymbol{E}^{(0)}(\boldsymbol{x},\boldsymbol{y}) \, \mathrm{d}S_{\boldsymbol{y}} = \left\langle \boldsymbol{E}^{(0)}(\boldsymbol{x},\cdot) \right\rangle \\ \boldsymbol{H}(\boldsymbol{x}) = \dfrac{1}{|Y|} \iint\limits_Y \boldsymbol{H}^{(0)}(\boldsymbol{x},\boldsymbol{y}) \, \mathrm{d}S_{\boldsymbol{y}} = \left\langle \boldsymbol{H}^{(0)}(\boldsymbol{x},\cdot) \right\rangle \end{cases}$$

where the average $\langle \cdot \rangle$ over the unit cell Y has been introduced.

Insert this form of the solution in the divergence equations in (6), and we get

$$\nabla_{\boldsymbol{y}} \cdot \{ \epsilon(\boldsymbol{y},x_3) \nabla_{\boldsymbol{y}} \Phi(\boldsymbol{x},\boldsymbol{y}) \} = -\nabla_{\boldsymbol{y}} \cdot \{ \epsilon(\boldsymbol{y},x_3) \boldsymbol{E}(\boldsymbol{x}) \} = -\nabla_{\boldsymbol{y}} \epsilon(\boldsymbol{y},x_3) \cdot \boldsymbol{E}(\boldsymbol{x})$$

which suggests a solution Φ of the separated form

$$\nabla_{\boldsymbol{y}}\Phi(\boldsymbol{x},\boldsymbol{y}) = -\nabla_{\boldsymbol{y}}\boldsymbol{\chi}^e(\boldsymbol{y},x_3)\cdot\boldsymbol{E}(\boldsymbol{x}) = -\nabla_{\boldsymbol{y}}\boldsymbol{\chi}^e(\boldsymbol{y},x_3)\cdot\boldsymbol{E}_t(\boldsymbol{x})$$

where $\boldsymbol{\chi}^e(\boldsymbol{y},x_3) = \chi_1^e(\boldsymbol{y},x_3)\hat{\boldsymbol{e}}_1 + \chi_2^e(\boldsymbol{y},x_3)\hat{\boldsymbol{e}}_2$, and $\chi_j^e(\boldsymbol{y},x_3)$, $j=1,2$, solves the local problem defined as the solution $\chi_j^e(\boldsymbol{y}) = \chi_j^e(\boldsymbol{y},x_3)$ to the following uniquely soluble boundary value problem for fixed $x_3 \in]h_-,h_+[$

$$\begin{cases} \nabla_{\boldsymbol{y}}\cdot\Big(\epsilon(\boldsymbol{y},x_3)\Big(\nabla_{\boldsymbol{y}}\chi_j^e(\boldsymbol{y}) - \hat{\boldsymbol{e}}_j\Big)\Big) = 0 \\ \chi_j^e(\boldsymbol{y}) \text{ continuous on } x_3 = h(\boldsymbol{y}) \\ \epsilon(\boldsymbol{y},x_3)\hat{\boldsymbol{n}}\cdot\Big(\nabla_{\boldsymbol{y}}\chi_j^e(\boldsymbol{y}) - \hat{\boldsymbol{e}}_j\Big) \text{ continuous on } x_3 = h(\boldsymbol{y}) \qquad j=1,2 \\ \chi_j^e(\boldsymbol{y}) \ Y\text{-periodic} \\ \Big\langle \chi_j^e \Big\rangle = 0 \end{cases}$$

Finally, the first order field contributions are

$$\begin{cases} \boldsymbol{E}^{(0)}(\boldsymbol{x},\boldsymbol{y}) = (\mathbf{I}_3 - \nabla_{\boldsymbol{y}}\boldsymbol{\chi}^e(\boldsymbol{y},x_3))\cdot\boldsymbol{E}(\boldsymbol{x}) \\ \boldsymbol{H}^{(0)}(\boldsymbol{x},\boldsymbol{y}) = \big(\mathbf{I}_3 - \nabla_{\boldsymbol{y}}\boldsymbol{\chi}^h(\boldsymbol{y},x_3)\big)\cdot\boldsymbol{H}(\boldsymbol{x}) \end{cases}$$

In the special case of piecewise constant permittivity, we have

$$\begin{cases} \nabla_{\boldsymbol{y}}^2\chi_j^e(\boldsymbol{y},x_3) = 0, \quad x_3 \neq h(\boldsymbol{y}) \\ \chi_j^e(\boldsymbol{y},x_3) \text{ continuous on } x_3 = h(\boldsymbol{y}) \\ \epsilon(\boldsymbol{y},x_3)\hat{\boldsymbol{n}}\cdot\Big(\nabla_{\boldsymbol{y}}\chi_j^e(\boldsymbol{y},x_3) - \hat{\boldsymbol{e}}_j\Big) \text{ continuous on } x_3 = h(\boldsymbol{y}) \quad j=1,2 \\ \chi_j^e(\boldsymbol{y},x_3) \ Y\text{-periodic} \\ \Big\langle \chi_j^e \Big\rangle = 0 \end{cases}$$

The magnetic problem is solved in a similar fashion by the solution of a local problem in $\boldsymbol{\chi}^h(\boldsymbol{y},x_3)$.

3.3. Second Order Term, $j=0$

The next order is $j=0$ and is somewhat more complex to analyze and provides explicit expressions of the homogenized material parameters. The divergence equations in (4) are

$$\begin{cases} \nabla_{\boldsymbol{y}}\cdot\Big\{\epsilon(\boldsymbol{y},x_3)\boldsymbol{E}^{(1)}(\boldsymbol{x},\boldsymbol{y})\Big\} = -\nabla_{\boldsymbol{x}}\cdot\Big\{\epsilon(\boldsymbol{y},x_3)\boldsymbol{E}^{(0)}(\boldsymbol{x},\boldsymbol{y})\Big\} \\ \nabla_{\boldsymbol{y}}\cdot\Big\{\mu(\boldsymbol{y},x_3)\boldsymbol{H}^{(1)}(\boldsymbol{x},\boldsymbol{y})\Big\} = -\nabla_{\boldsymbol{x}}\cdot\Big\{\mu(\boldsymbol{y},x_3)\boldsymbol{H}^{(0)}(\boldsymbol{x},\boldsymbol{y})\Big\} \end{cases}$$

and the boundary conditions (5) are

$$\begin{cases} \left[\epsilon(\boldsymbol{y},x_3)\left(\nabla_{\boldsymbol{y}}h(\boldsymbol{y})\cdot\boldsymbol{E}_t^{(1)}(\boldsymbol{x},\boldsymbol{y})-E_3^{(0)}(\boldsymbol{x})\right)\right]=0 \\ \left[\mu(\boldsymbol{y},x_3)\left(\nabla_{\boldsymbol{y}}h(\boldsymbol{y})\cdot\boldsymbol{H}_t^{(1)}(\boldsymbol{x},\boldsymbol{y})-H_3^{(0)}(\boldsymbol{x})\right)\right]=0 \end{cases} \qquad x_3=h(\boldsymbol{y})$$

Integrate the divergence equations over the unit cell (over Y_+ and Y_-, which depend on x_3) and pay special attention to any contributions from the boundary curve C. We get ($\boldsymbol{E}^{(1)}(\boldsymbol{x},\boldsymbol{y})$ is assumed Y-periodic, and $\hat{\boldsymbol{n}}$ is the outwardly pointing unit normal vector to C, into the region Y_+, and the integration along $C(x_3)$ is in the counter wise direction in the $\hat{\boldsymbol{e}}_1$-$\hat{\boldsymbol{e}}_2$-plane), see also Lemma A.1 in Appendix A

$$\begin{aligned}
&-\int_C \hat{\boldsymbol{n}}\cdot\left[\epsilon(\boldsymbol{y},x_3)\boldsymbol{E}^{(1)}(\boldsymbol{x},\boldsymbol{y})\right]\,\mathrm{d}l_{\boldsymbol{y}} \\
&=\iint_{Y_+}\nabla_{\boldsymbol{y}}\cdot\left\{\epsilon(\boldsymbol{y},x_3)\boldsymbol{E}^{(1)}(\boldsymbol{x},\boldsymbol{y})\right\}\,\mathrm{d}S_{\boldsymbol{y}} \\
&\quad+\iint_{Y_-}\nabla_{\boldsymbol{y}}\cdot\left\{\epsilon(\boldsymbol{y},x_3)\boldsymbol{E}^{(1)}(\boldsymbol{x},\boldsymbol{y})\right\}\,\mathrm{d}S_{\boldsymbol{y}} \\
&=-\iint_{Y_+}\nabla_{\boldsymbol{x}}\cdot\left\{\epsilon(\boldsymbol{y},x_3)\boldsymbol{E}^{(0)}(\boldsymbol{x},\boldsymbol{y})\right\}\,\mathrm{d}S_{\boldsymbol{y}} \\
&\quad-\iint_{Y_-}\nabla_{\boldsymbol{x}}\cdot\left\{\epsilon(\boldsymbol{y},x_3)\boldsymbol{E}^{(0)}(\boldsymbol{x},\boldsymbol{y})\right\}\,\mathrm{d}S_{\boldsymbol{y}} \\
&=-\nabla_{\boldsymbol{x}}\cdot\langle\{\epsilon(\boldsymbol{y},x_3)\left(\mathbf{I}_2-\nabla_{\boldsymbol{y}}\boldsymbol{\chi}^e(\boldsymbol{y},x_3)\right)\}\rangle\cdot\boldsymbol{E}(\boldsymbol{x}) \\
&\quad-\iint_{Y_+}\frac{\partial}{\partial x_3}\left\{\epsilon_+E_3^{(0)}(\boldsymbol{x})\right\}\,\mathrm{d}S_{\boldsymbol{y}} \\
&\quad-\iint_{Y_-}\frac{\partial}{\partial x_3}\left\{\epsilon_-E_3^{(0)}(\boldsymbol{x})\right\}\,\mathrm{d}S_{\boldsymbol{y}} \\
&=-\nabla_{\boldsymbol{x}}\cdot\left\{\boldsymbol{\epsilon}^h(x_3)\cdot\boldsymbol{E}(\boldsymbol{x})\right\}+E_3^{(0)}(\boldsymbol{x})\,[\epsilon]\int_C\frac{1}{|\nabla_{\boldsymbol{y}}h(\boldsymbol{y})|}\,\mathrm{d}l_{\boldsymbol{y}}
\end{aligned}$$

where $[\epsilon]=\epsilon_+-\epsilon_-$ and where we have introduced the homogenized

permittivity

$$\boldsymbol{\epsilon}^h(x_3) = \frac{1}{|Y|} \iint_Y \epsilon(\boldsymbol{y}, x_3) \left(\mathbf{I}_3 - \nabla_{\boldsymbol{y}} \boldsymbol{\chi}^e(\boldsymbol{y})\right) \, \mathrm{d}S_{\boldsymbol{y}}$$

The left hand side is rewritten, due to the boundary conditions, and we get

$$\begin{aligned} -\int_C \hat{\boldsymbol{n}} \cdot \left[\epsilon(\boldsymbol{y}, x_3) \boldsymbol{E}^{(1)}(\boldsymbol{x}, \boldsymbol{y})\right] \, \mathrm{d}l_{\boldsymbol{y}} &= \int_C \frac{[\epsilon(\boldsymbol{y}, x_3)] \, E_3^{(0)}(\boldsymbol{x})}{|\nabla_{\boldsymbol{y}} h(\boldsymbol{y})|} \, \mathrm{d}l_{\boldsymbol{y}} \\ &= E_3^{(0)}(\boldsymbol{x}) \, [\epsilon] \int_C \frac{1}{|\nabla_{\boldsymbol{y}} h(\boldsymbol{y})|} \, \mathrm{d}l_{\boldsymbol{y}} \end{aligned}$$

and we obtain

$$\nabla_{\boldsymbol{x}} \cdot \left\{ \boldsymbol{\epsilon}^h(x_3) \cdot \boldsymbol{E}(\boldsymbol{x}) \right\} = 0$$

A similar treatment of the magnetic field gives the homogenized permeability

$$\boldsymbol{\mu}^h(x_3) = \frac{1}{|Y|} \iint_Y \mu(\boldsymbol{y}, x_3) \left(\mathbf{I}_3 - \nabla_{\boldsymbol{y}} \boldsymbol{\chi}^h(\boldsymbol{y})\right) \, \mathrm{d}S_{\boldsymbol{y}}$$

The effective (homogenized) parameters, $\boldsymbol{\epsilon}^h(x_3)$ and $\boldsymbol{\mu}^h(x_3)$, can also be written in terms of a line integral by an application of the Gauss' theorem in the plane. We have (the unit normal vector is as above pointing into the region Y_+ and the integration along $C(x_3)$ is in the counter wise direction in the $\hat{\boldsymbol{e}}_1$-$\hat{\boldsymbol{e}}_2$-plane)

$$\begin{cases} \boldsymbol{\epsilon}^h(x_3) = \dfrac{1}{|Y|} \Big(\left(\epsilon_+ |Y_+|(x_3) + \epsilon_- |Y_-|(x_3)\right) \mathbf{I}_3 \\ \qquad\qquad + (\epsilon_+ - \epsilon_-) \displaystyle\int_{C(x_3)} \hat{\boldsymbol{n}} \boldsymbol{\chi}^e(\boldsymbol{y}, x_3) \, \mathrm{d}l_{\boldsymbol{y}} \Big) \\ \boldsymbol{\mu}^h(x_3) = \dfrac{1}{|Y|} \Big(\left(\mu_+ |Y_+|(x_3) + \mu_- |Y_-|(x_3)\right) \mathbf{I}_3 \\ \qquad\qquad + (\mu_+ - \mu_-) \displaystyle\int_{C(x_3)} \hat{\boldsymbol{n}} \boldsymbol{\chi}^h(\boldsymbol{y}, x_3) \, \mathrm{d}l_{\boldsymbol{y}} \Big) \end{cases}$$

We now proceed with the curl equations (4), which are

$$\begin{cases} \nabla_{\boldsymbol{x}} \times \boldsymbol{E}^{(0)}(\boldsymbol{x}, \boldsymbol{y}) + \nabla_{\boldsymbol{y}} \times \boldsymbol{E}^{(1)}(\boldsymbol{x}, \boldsymbol{y}) = \mathrm{i}k_0 \mu(\boldsymbol{y}, x_3) \boldsymbol{H}^{(0)}(\boldsymbol{x}, \boldsymbol{y}) \\ \nabla_{\boldsymbol{x}} \times \boldsymbol{H}^{(0)}(\boldsymbol{x}, \boldsymbol{y}) + \nabla_{\boldsymbol{y}} \times \boldsymbol{H}^{(1)}(\boldsymbol{x}, \boldsymbol{y}) = -\mathrm{i}k_0 \epsilon(\boldsymbol{y}, x_3) \boldsymbol{E}^{(0)}(\boldsymbol{x}, \boldsymbol{y}) \end{cases}$$

and the boundary conditions are, see (5)

$$\begin{cases} \Big[\nabla_{\boldsymbol{y}} h(\boldsymbol{y}) \times \boldsymbol{E}^{(1)}(\boldsymbol{x},\boldsymbol{y}) - \hat{\boldsymbol{e}}_3 \times \boldsymbol{E}_t^{(0)}(\boldsymbol{x},\boldsymbol{y})\Big] = \boldsymbol{0} \\ \Big[\nabla_{\boldsymbol{y}} h(\boldsymbol{y}) \times \boldsymbol{H}^{(1)}(\boldsymbol{x},\boldsymbol{y}) - \hat{\boldsymbol{e}}_3 \times \boldsymbol{H}_t^{(0)}(\boldsymbol{x},\boldsymbol{y})\Big] = \boldsymbol{0} \end{cases} \qquad x_3 = h(\boldsymbol{y})$$

The first line in the boundary conditions is split into its horizontal and vertical components. The result is

$$\begin{cases} \hat{\boldsymbol{e}}_3 \times \Big[\nabla_{\boldsymbol{y}} h(\boldsymbol{y}) E_3^{(1)}(\boldsymbol{x},\boldsymbol{y}) + \boldsymbol{E}_t^{(0)}(\boldsymbol{x},\boldsymbol{y})\Big] = \boldsymbol{0} \\ \hat{\boldsymbol{e}}_3 \cdot \Big[\nabla_{\boldsymbol{y}} h(\boldsymbol{y}) \times \boldsymbol{E}_t^{(1)}(\boldsymbol{x},\boldsymbol{y})\Big] = \boldsymbol{0} \end{cases} \qquad x_3 = h(\boldsymbol{y})$$

Integrate the curl equations over the unit cell (over Y_+ and Y_-, which depend on x_3) and pay special attention to any contributions from the boundary curve C. We get ($\boldsymbol{E}^{(1)}(\boldsymbol{x},\boldsymbol{y})$ is assumed Y-periodic, and the unit normal vector $\hat{\boldsymbol{n}}$ is as above pointing into the region Y_+ and the integration along $C(x_3)$ is in the counter wise direction in the $\hat{\boldsymbol{e}}_1$-$\hat{\boldsymbol{e}}_2$-plane)

$$\begin{aligned} &\iint\limits_{Y_+} \nabla_{\boldsymbol{x}} \times \Big\{\boldsymbol{E}^{(0)}(\boldsymbol{x},\boldsymbol{y})\Big\}\, \mathrm{d}S_{\boldsymbol{y}} + \iint\limits_{Y_-} \nabla_{\boldsymbol{x}} \times \Big\{\boldsymbol{E}^{(0)}(\boldsymbol{x},\boldsymbol{y})\Big\}\, \mathrm{d}S_{\boldsymbol{y}} \\ &+ \iint\limits_{Y_+} \nabla_{\boldsymbol{y}} \times \Big\{\boldsymbol{E}^{(1)}(\boldsymbol{x},\boldsymbol{y})\Big\}\, \mathrm{d}S_{\boldsymbol{y}} + \iint\limits_{Y_-} \nabla_{\boldsymbol{y}} \times \Big\{\boldsymbol{E}^{(1)}(\boldsymbol{x},\boldsymbol{y})\Big\}\, \mathrm{d}S_{\boldsymbol{y}} \\ &= \mathrm{i}k_0 \Big\langle \mu(\boldsymbol{y},x_3)\Big(\mathbf{I}_3 - \nabla_{\boldsymbol{y}} \boldsymbol{\chi}^h(\boldsymbol{y},x_3)\Big)\Big\rangle \cdot \boldsymbol{H}(\boldsymbol{x}) = \mathrm{i}k_0 \boldsymbol{\mu}^h(x_3) \cdot \boldsymbol{H}(\boldsymbol{x}) \end{aligned}$$

or

$$\begin{aligned} \nabla_{\boldsymbol{x}} \times \boldsymbol{E}(\boldsymbol{x}) - \hat{\boldsymbol{e}}_3 \times &\int\limits_C \frac{\Big[\boldsymbol{E}_t^{(0)}(\boldsymbol{x},\boldsymbol{y})\Big]}{|\nabla_{\boldsymbol{y}} h(\boldsymbol{y})|}\, \mathrm{d}l_{\boldsymbol{y}} \\ &- \int\limits_C \hat{\boldsymbol{n}} \times \Big[\boldsymbol{E}^{(1)}(\boldsymbol{x},\boldsymbol{y})\Big]\, \mathrm{d}l_{\boldsymbol{y}} = \mathrm{i}k_0 \boldsymbol{\mu}^h(x_3) \cdot \boldsymbol{H}(\boldsymbol{x}) \end{aligned}$$

The line integral is simplified by the use of the boundary conditions. We get

$$\int\limits_C \hat{\boldsymbol{n}} \times \Big[\boldsymbol{E}^{(1)}(\boldsymbol{x},\boldsymbol{y})\Big]\, \mathrm{d}l_{\boldsymbol{y}} = -\int\limits_C \frac{\hat{\boldsymbol{e}}_3 \times \Big[\boldsymbol{E}_t^{(0)}(\boldsymbol{x},\boldsymbol{y})\Big]}{|\nabla_{\boldsymbol{y}} h(\boldsymbol{y})|}\, \mathrm{d}l_{\boldsymbol{y}}$$

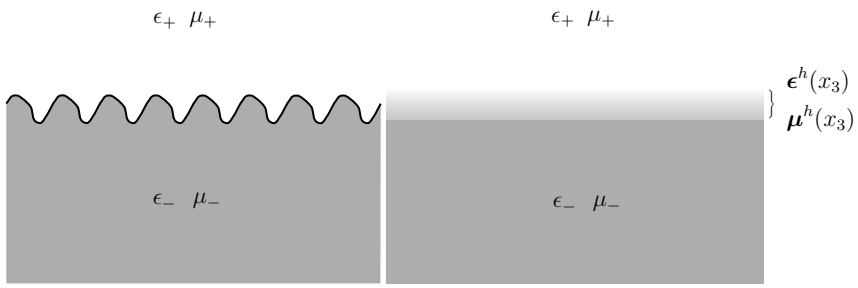

Figure 2. The original material (left) and the homogenized material (right).

We finally get

$$\nabla_{\boldsymbol{x}} \times \boldsymbol{E}(\boldsymbol{x}) = \mathrm{i}k_0 \boldsymbol{\mu}^h(x_3) \cdot \boldsymbol{H}(\boldsymbol{x})$$

Similarly, for the curl of the magnetic field holds

$$\nabla_{\boldsymbol{x}} \times \boldsymbol{H}(\boldsymbol{x}) = -\mathrm{i}k_0 \boldsymbol{\epsilon}^h(x_3) \cdot \boldsymbol{E}(\boldsymbol{x})$$

3.4. Main Theorem of Homogenization

In the preceding section we showed that the corrugated surface, in the limit of vanishing periodicity, is equivalent to an inhomogeneous transition region or slab, with permittivity $\boldsymbol{\epsilon}^h(x_3)$ and permeability $\boldsymbol{\mu}^h(x_3)$ as illustrated in Figure 2. The explicit permittivity and permeability dyadics, $\boldsymbol{\epsilon}^h(x_3)$ and $\boldsymbol{\mu}^h(x_3)$, of the slab were also found. In this section we collect the main result of the paper given by the following theorem:

Theorem. *The scaled problem, i.e., $x_3 = h(x_1/\varepsilon, x_2/\varepsilon)$ (Y^ε-periodic surface in $\mathbb{R}^2$), converges in the limit $\varepsilon \to 0$ to the following Maxwell equations in the region $x_3 \in]h_-, h_+[$*

$$\begin{cases} \nabla \cdot \big(\boldsymbol{\epsilon}^h(x_3) \cdot \boldsymbol{E}(\boldsymbol{x})\big) = 0 \\ \nabla \cdot \big(\boldsymbol{\mu}^h(x_3) \cdot \boldsymbol{H}(\boldsymbol{x})\big) = 0 \end{cases}$$

and

$$\begin{cases} \nabla \times \boldsymbol{E}(\boldsymbol{x}) = \mathrm{i}k_0 \boldsymbol{\mu}^h(x_3) \cdot \boldsymbol{H}(\boldsymbol{x}) \\ \nabla \times \boldsymbol{H}(\boldsymbol{x}) = -\mathrm{i}k_0 \boldsymbol{\epsilon}^h(x_3) \cdot \boldsymbol{E}(\boldsymbol{x}) \end{cases}$$

where ($\mathrm{d}S_{\boldsymbol{y}} = \mathrm{d}y_1\mathrm{d}y_2$)

$$\begin{cases} \boldsymbol{\epsilon}^h(x_3) = \dfrac{1}{|Y|}\displaystyle\iint_Y \epsilon(\boldsymbol{y}, x_3)\left(\mathbf{I}_3 - \nabla_{\boldsymbol{y}}\boldsymbol{\chi}^e(\boldsymbol{y})\right)\,\mathrm{d}S_{\boldsymbol{y}} \\ \boldsymbol{\mu}^h(x_3) = \dfrac{1}{|Y|}\displaystyle\iint_Y \mu(\boldsymbol{y}, x_3)\left(\mathbf{I}_3 - \nabla_{\boldsymbol{y}}\boldsymbol{\chi}^h(\boldsymbol{y})\right)\,\mathrm{d}S_{\boldsymbol{y}} \end{cases} \tag{7}$$

The vector-valued function $\boldsymbol{\chi}^e(\boldsymbol{y}, x_3) = \chi_1^e(\boldsymbol{y}, x_3)\hat{\boldsymbol{e}}_1 + \chi_2^e(\boldsymbol{y}, x_3)\hat{\boldsymbol{e}}_2$ *solves the local problem*

$$\begin{cases} \nabla_{\boldsymbol{y}} \cdot \left(\epsilon(\boldsymbol{y}, x_3)\left(\nabla_{\boldsymbol{y}}\chi_j^e(\boldsymbol{y}) - \hat{\boldsymbol{e}}_j\right)\right) = 0 \\ \chi_j^e(\boldsymbol{y}) \text{ continuous on } x_3 = h(\boldsymbol{y}) \\ \epsilon(\boldsymbol{y}, x_3)\hat{\boldsymbol{n}} \cdot \left(\nabla_{\boldsymbol{y}}\chi_j^e(\boldsymbol{y}) - \hat{\boldsymbol{e}}_j\right) \text{ continuous on } x_3 = h(\boldsymbol{y}) \qquad j = 1, 2 \\ \chi_j^e(\boldsymbol{y}) \ Y\text{-periodic} \\ \left\langle \chi_j^e \right\rangle = 0 \end{cases} \tag{8}$$

Outside the slab $x_3 \in [h_-, h_+]$ *the permittivity is* $\boldsymbol{\epsilon}^h(x_3) = \mathbf{I}_3\epsilon_\pm$, *respectively. A similar local problem holds for the magnetic field.*

Note that the results presented by Nevard and Keller [13] have two extra terms in the curl equations. These terms should not be present.

We conclude that the effective permittivity, $\boldsymbol{\epsilon}^h(x_3)$, and permeability, $\boldsymbol{\mu}^h(x_3)$, both have the form

$$\begin{pmatrix} A_{11} & A_{12} & 0 \\ A_{21} & A_{22} & 0 \\ 0 & 0 & A_{33} \end{pmatrix}$$

in a Cartesian coordinate representation of the effective permittivity and permeability dyadics. The 33-component has always the form

$$\epsilon_{33}^h = \langle \epsilon(\cdot, x_3) \rangle\,, \qquad \mu_{33}^h = \langle \mu(\cdot, x_3) \rangle$$

where the average over the unit cell Y is

$$\langle f(\cdot) \rangle = \frac{1}{|Y|}\iint_Y f(\boldsymbol{y})\,\mathrm{d}S_{\boldsymbol{y}}$$

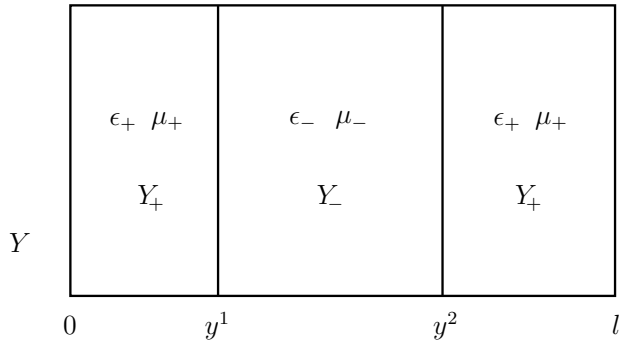

Figure 3. The unit cell for a surface with two-dimensional corrugations.

4. ONE-DIMENSIONAL INTERFACE PROBLEM

There are considerable simplifications to be made if the corrugations of the surface are only in one dimension, *i.e.*, $x_3 = h(y_1)$ (with cross section as in Figure 1a)). In this section we investigate these simplifications in more details.

We assume there are two regions in the unit cell, Y_+ and Y_-, with boundary located at y^1 and y^2, respectively (we assume Y_+ is the two intervals $]0, y^1[\cup]y^2, l_1[$ and Y_- is the interval $]y^1, y^2[$), see Figure 3. These boundary locations depend on x_3. Generalizations to more complex geometries are straightforward.

The local problem in one dimension is easily solved. The solution is ($|Y| = l_1$, $|Y_+| = l_1 + y^1 - y^2$ and $|Y_-| = y^2 - y^1$)

$$\chi_1^e(y_1, x_3) = \begin{cases} \dfrac{|Y_-|\left(2y_1 - y^1 + |Y| - y^2\right)(\epsilon_+ - \epsilon_-)}{2|Y_+|\epsilon_- + 2|Y_-|\epsilon_+}, & 0 < y_1 < y^1 \\ \dfrac{|Y_+|\left(y^1 + y^2 - 2y_1\right)(\epsilon_+ - \epsilon_-)}{2|Y_+|\epsilon_- + 2|Y_-|\epsilon_+}, & y^1 < y_1 < y^2 \\ \dfrac{|Y_-|\left(2y_1 - y^1 - |Y| - y^2\right)(\epsilon_+ - \epsilon_-)}{2|Y_+|\epsilon_- + 2|Y_-|\epsilon_+}, & y^2 < y_1 < l_1 \end{cases}$$

and consequently

$$\frac{\partial \chi_1^e(y_1, x_3)}{\partial y_1} = \pm |Y_\mp| \frac{\epsilon_+ - \epsilon_-}{|Y_+|\epsilon_- + |Y_-|\epsilon_+}, \qquad y_1 \in Y_\pm$$

The second component $\chi_2^e =$ constant, where the value of the constant is immaterial.

The effective permittivity, given by (7), can be written as

$$\epsilon_{11}^h(x_3) = \frac{\epsilon_+|Y_+(x_3)|}{|Y|} + \frac{\epsilon_-|Y_-(x_3)|}{|Y|} - \frac{|Y_+||Y_-|\left(\epsilon_+ - \epsilon_-\right)^2}{|Y|\left(|Y_+|\epsilon_- + |Y_-|\epsilon_+\right)}$$

which we rewrite as

$$\epsilon_{11}^h(x_3) = \frac{|Y|}{|Y_+(x_3)|/\epsilon_+ + |Y_-(x_3)|/\epsilon_-}$$

since

$$\begin{aligned}\epsilon_{11}^h &= \frac{1}{|Y|}\left(\epsilon_+|Y_+| + \epsilon_-|Y_-| - \frac{|Y_+||Y_-|\left(\epsilon_+ - \epsilon_-\right)^2}{|Y_+|\epsilon_- + |Y_-|\epsilon_+}\right) \\ &= \frac{\epsilon_+\epsilon_-\left(|Y_+|^2 + |Y_-|^2 + 2|Y_+||Y_-|\right)}{|Y|\left(|Y_+|\epsilon_- + |Y_-|\epsilon_+\right)} = \frac{\epsilon_+\epsilon_-|Y|}{|Y_+|\epsilon_- + |Y_-|\epsilon_+}\end{aligned}$$

The other two non-zero components of the effective permittivity are trivial averages.

$$\epsilon_{22}^h(x_3) = \epsilon_{33}^h(x_3) = \frac{\epsilon_+|Y_+(x_3)|}{|Y|} + \frac{\epsilon_-|Y_-(x_3)|}{|Y|}$$

The result can be summarized in

$$\epsilon_{ij}^h(x_3) = \begin{pmatrix} \frac{1}{\langle 1/\epsilon\rangle(x_3)} & 0 & 0 \\ 0 & \langle\epsilon\rangle(x_3) & 0 \\ 0 & 0 & \langle\epsilon\rangle(x_3) \end{pmatrix} \tag{9}$$

The solution to the corresponding magnetic homogenization problem is

$$\mu_{ij}^h(x_3) = \begin{pmatrix} \frac{1}{\langle 1/\mu\rangle(x_3)} & 0 & 0 \\ 0 & \langle\mu\rangle(x_3) & 0 \\ 0 & 0 & \langle\mu\rangle(x_3) \end{pmatrix}$$

The lowest order electric field is

$$\begin{aligned}\boldsymbol{E}^{(0)}(\boldsymbol{x},\boldsymbol{y}) &= \left(\mathbf{I}_3 - \nabla_{\boldsymbol{y}}\boldsymbol{\chi}^e(\boldsymbol{y},x_3)\right)\cdot\boldsymbol{E}(\boldsymbol{x}) \\ &= \left(\mathbf{I}_3 \mp |Y_\mp|\frac{\epsilon_+ - \epsilon_-}{|Y_+|\epsilon_- + |Y_-|\epsilon_+}\hat{\boldsymbol{e}}_1\hat{\boldsymbol{e}}_1\right)\cdot\boldsymbol{E}(\boldsymbol{x}) \qquad y_1 \in Y_\pm \\ &= \frac{\epsilon_\mp|Y|}{|Y_+|\epsilon_- + |Y_-|\epsilon_+}\hat{\boldsymbol{e}}_1E_1(\boldsymbol{x}) + \hat{\boldsymbol{e}}_2E_2(\boldsymbol{x}) + \hat{\boldsymbol{e}}_3E_3(\boldsymbol{x})\end{aligned}$$

4.1. Perfectly Conducting Boundary as a Limit Case

The limit values of the effective permittivity and the fields as the lower material becomes a perfectly conducting material is of interest. It is important to realize that the perfectly conducting case already is a limit of vanishing penetration depth. Since the homogenization also is a limit process, the question whether these limits commute or not has been debated [2, 11, 14, 15].

In this paper we present the limit of a perfectly boundary by letting $\epsilon_- \to \infty$. The effective permittivity in the slab $x_3 \in]h_-, h_+[$ then becomes

$$\epsilon^h_{ij}(x_3) = \begin{pmatrix} \epsilon_+ \dfrac{|Y|}{|Y_+(x_3)|} & 0 & 0 \\ 0 & \infty & 0 \\ 0 & 0 & \infty \end{pmatrix}$$

and the lowest order electric field is

$$\boldsymbol{E}^{(0)}(\boldsymbol{x}, \boldsymbol{y}) = \begin{Bmatrix} \dfrac{|Y|}{|Y_+|} \\ 0 \end{Bmatrix} \hat{\boldsymbol{e}}_1 E_1(\boldsymbol{x}) + \hat{\boldsymbol{e}}_2 E_2(\boldsymbol{x}) + \hat{\boldsymbol{e}}_3 E_3(\boldsymbol{x}), \qquad y_1 \in Y_\pm$$

5. PROPAGATORS AND SURFACE IMPEDANCE DYADIC

As a result of the homogenization analysis above, the action of the corrugated surface is equivalent to an inhomogeneous transition region. This inhomogeneous transition region, $x_3 \in]h_-, h_+[$, can be characterized with an effective surface impedance, $\mathbf{Z}$, or a reflection dyadic, $\mathbf{r}$, if the incidence field is a plane wave from above (the region $x_3 > h_+$). The incident direction of this plane wave is parameterized by its horizontal wave vector $\boldsymbol{k}_t$ (spatial Fourier variable in the $\hat{\boldsymbol{e}}_1$-$\hat{\boldsymbol{e}}_2$-plane). The angle of incidence is determined by the size and the direction of this wave vector. Specifically, the length determines the angle of incidence θ_+ (and the angle of transmission θ_-), *i.e.*, $k_t = |\boldsymbol{k}_t| = k_\pm \sin\theta_\pm$, where $k_\pm = \omega\sqrt{\epsilon_0\mu_0\epsilon_\pm\mu_\pm}$. The direction of $\boldsymbol{k}_t$ in the $\hat{\boldsymbol{e}}_1$-$\hat{\boldsymbol{e}}_2$-plane determines the azimuthal direction ϕ of the incident wave, *i.e.*, $\boldsymbol{k}_t = k_t(\cos\phi\hat{\boldsymbol{e}}_1 + \sin\phi\hat{\boldsymbol{e}}_2)$.

5.1. Surface Impedance

The relation between the horizontal components of the electric and magnetic fields $\boldsymbol{E}_t$ and $\boldsymbol{H}_t$, respectively, at $x_3 = h_+$, is characterized

by the surface impedance dyadic $\mathbf{Z}$ defined as

$$\boldsymbol{E}_t(h_+) = \eta_0 \mathbf{Z} \cdot (\hat{\boldsymbol{e}}_3 \times \boldsymbol{H}_t(h_+)) = \eta_0 \mathbf{Z} \cdot \mathbf{J} \cdot \boldsymbol{H}_t(h_+)$$

where $\mathbf{J} = \hat{\boldsymbol{e}}_3 \times \mathbf{I}_3 = \hat{\boldsymbol{e}}_3 \times \mathbf{I}_2$ denotes a projection onto the $\hat{\boldsymbol{e}}_1$-$\hat{\boldsymbol{e}}_2$-plane followed by a rotation of $\pi/2$ in the $\hat{\boldsymbol{e}}_1$-$\hat{\boldsymbol{e}}_2$-plane. The identity dyadic in $\mathbb{R}^2$ and $\mathbb{R}^3$ are denoted $\mathbf{I}_2$ and $\mathbf{I}_3$, respectively.

The propagators, $\mathbf{P}_{ij}(h_+, h_-)$, $i, j = 1, 2$, of the inhomogeneous slab, $x_3 \in]h_-, h_+[$, relate the field at the top and bottom of the slab. They are defined as

$$\begin{pmatrix} \boldsymbol{E}_t(h_+) \\ \eta_0 \mathbf{J} \cdot \boldsymbol{H}_t(h_+) \end{pmatrix} = \begin{pmatrix} \mathbf{P}_{11}(h_+, h_-) & \mathbf{P}_{12}(h_+, h_-) \\ \mathbf{P}_{21}(h_+, h_-) & \mathbf{P}_{22}(h_+, h_-) \end{pmatrix} \cdot \begin{pmatrix} \boldsymbol{E}_t(h_-) \\ \eta_0 \mathbf{J} \cdot \boldsymbol{H}_t(h_-) \end{pmatrix} \tag{10}$$

Efficient methods for analytical or numerical computation algorithms of these propagators are found in *e.g.*, [8, 9, 16].

5.1.1. Perfectly Conducting Backing

If the lower surface of the inhomogeneous transition region is perfectly conducting the tangential electric field is zero, *i.e.*, $\boldsymbol{E}_t(h_-) = \mathbf{0}$, and we get from (10)

$$\begin{aligned} \boldsymbol{E}_t(h_+) &= \mathbf{P}_{12}(h_+, h_-) \cdot \eta_0 \mathbf{J} \cdot \boldsymbol{H}_t(h_-) \\ &= \mathbf{P}_{12}(h_+, h_-) \cdot \mathbf{P}_{22}^{-1}(h_+, h_-) \cdot \eta_0 \mathbf{J} \cdot \boldsymbol{H}_t(h_+) \end{aligned}$$

This is an exact relation between the tangential electric and magnetic fields on the upper part of the slab if the lower material has a perfectly conducting backing. This then gives the explicit expression of the surface impedance dyadic of the slab.

$$\mathbf{Z} = \mathbf{P}_{12}(h_+, h_-) \cdot \mathbf{P}_{22}^{-1}(h_+, h_-) \tag{11}$$

5.1.2. Dielectric Backing

We now address the penetrable case, and assume there are sources only above the interface. In the region below the transition region the fields satisfy a radiation condition which is most conveniently expressed with the wave splitting concept defined as [16]

$$\begin{pmatrix} \boldsymbol{F}^+(\boldsymbol{k}_t, z) \\ \boldsymbol{F}^-(\boldsymbol{k}_t, z) \end{pmatrix} = \frac{1}{2} \begin{pmatrix} \mathbf{I}_2 & -\mathbf{W}^-(\boldsymbol{k}_t) \\ \mathbf{I}_2 & \mathbf{W}^-(\boldsymbol{k}_t) \end{pmatrix} \cdot \begin{pmatrix} \boldsymbol{E}_t(\boldsymbol{k}_t, z) \\ \eta_0 \mathbf{J} \cdot \boldsymbol{H}_t(\boldsymbol{k}_t, z) \end{pmatrix} \tag{12}$$

where

$$\mathbf{W}^-(\boldsymbol{k}_t) = \hat{\boldsymbol{e}}_\parallel\hat{\boldsymbol{e}}_\parallel\frac{\left(k_-^2 - k_t^2\right)^{1/2}}{k_-} + \hat{\boldsymbol{e}}_\perp\hat{\boldsymbol{e}}_\perp\frac{k_-}{\left(k_-^2 - k_t^2\right)^{1/2}}$$
$$= \hat{\boldsymbol{e}}_\parallel\hat{\boldsymbol{e}}_\parallel\cos\theta_- + \frac{\hat{\boldsymbol{e}}_\perp\hat{\boldsymbol{e}}_\perp}{\cos\theta_-}$$

where $\hat{\boldsymbol{e}}_\parallel = \boldsymbol{k}_t/k_t = \cos\phi\hat{\boldsymbol{e}}_1 + \sin\phi\hat{\boldsymbol{e}}_2$ and $\hat{\boldsymbol{e}}_\perp = \mathbf{J}\cdot\hat{\boldsymbol{e}}_\parallel = \cos\phi\hat{\boldsymbol{e}}_2 - \sin\phi\hat{\boldsymbol{e}}_1$.

The appropriate radiation condition at the lower part of the transition region is $\boldsymbol{F}^+(h_-) = \mathbf{0}$ (only down-going waves) which implies

$$\boldsymbol{E}_t(h_-) = \mathbf{W}^-\cdot\eta_0\mathbf{J}\cdot\boldsymbol{H}_t(h_-)$$

Equation (10) then implies

$$\boldsymbol{E}_t(h_+) = \big(\mathbf{P}_{11}(h_+,h_-)\cdot\mathbf{W}^- + \mathbf{P}_{12}(h_+,h_-)\big)$$
$$\cdot\big(\mathbf{P}_{21}(h_+,h_-)\cdot\mathbf{W}^- + \mathbf{P}_{22}(h_+,h_-)\big)^{-1}\cdot\eta_0\mathbf{J}\cdot\boldsymbol{H}_t(h_+)$$

and the surface impedance dyadic can be identified as

$$\mathbf{Z} = \big(\mathbf{P}_{11}(h_+,h_-)\cdot\mathbf{W}^- + \mathbf{P}_{12}(h_+,h_-)\big)$$
$$\cdot\big(\mathbf{P}_{21}(h_+,h_-)\cdot\mathbf{W}^- + \mathbf{P}_{22}(h_+,h_-)\big)^{-1}$$

We observe that the perfectly conducting case, (11), is a special case of this general expression, *viz.*, $\mathbf{W}^- = \mathbf{0}$.

5.2. Reflection Dyadic

The reflection dyadic $\mathbf{r}$ of the slab can also be calculated. It relates the up- and down-going fields $\boldsymbol{F}^\pm$ at $x_3 = h_+$ by the use of a wave splitting similar to the one in (12), *i.e.*,

$$\boldsymbol{F}^+(\boldsymbol{k}_t,h_+) = \mathbf{r}\cdot\boldsymbol{F}^-(\boldsymbol{k}_t,h_+)$$

and

$$\begin{cases}\boldsymbol{E}_t(h_+) = \mathbf{r}\cdot\boldsymbol{F}^-(h_+) + \boldsymbol{F}^-(h_+)\\ \eta_0\mathbf{W}^+\cdot\mathbf{J}\cdot\boldsymbol{H}_t(h_+) = -\mathbf{r}\cdot\boldsymbol{F}^-(h_+) + \boldsymbol{F}^-(h_+)\end{cases}$$

where

$$\mathbf{W}^+(\boldsymbol{k}_t) = \hat{\boldsymbol{e}}_\parallel\hat{\boldsymbol{e}}_\parallel\frac{\left(k_+^2 - k_t^2\right)^{1/2}}{k_+} + \hat{\boldsymbol{e}}_\perp\hat{\boldsymbol{e}}_\perp\frac{k_+}{\left(k_+^2 - k_t^2\right)^{1/2}}$$
$$= \hat{\boldsymbol{e}}_\parallel\hat{\boldsymbol{e}}_\parallel\cos\theta_+ + \frac{\hat{\boldsymbol{e}}_\perp\hat{\boldsymbol{e}}_\perp}{\cos\theta_+} \tag{13}$$

We recombine these expressions to

$$\boldsymbol{E}_t(h_+) = (\mathbf{I}_2 + \mathbf{r}) \cdot (\mathbf{I}_2 - \mathbf{r})^{-1} \cdot \eta_0 \mathbf{W}^+ \cdot \mathbf{J} \cdot \boldsymbol{H}_t(h_+)$$

and the surface impedance can be expressed in the reflection dyadic as

$$\mathbf{Z} = (\mathbf{I}_2 + \mathbf{r}) \cdot (\mathbf{I}_2 - \mathbf{r})^{-1} \cdot \mathbf{W}^+$$

This expression can be inverted to find the reflection dyadic in the impedance dyadic. The result is

$$\mathbf{r} = -\left(\mathbf{I}_2 + \mathbf{Z} \cdot \mathbf{W}^{+-1}\right)^{-1} \cdot \left(\mathbf{I}_2 - \mathbf{Z} \cdot \mathbf{W}^{+-1}\right)$$

For a perfectly conducting backing, the impedance dyadic in (11) implies

$$\begin{aligned}\mathbf{r} = &-\left(\mathbf{I}_2 + \mathbf{P}_{12}(h_+, h_-) \cdot \mathbf{P}_{22}^{-1}(h_+, h_-) \cdot \mathbf{W}^{+-1}\right)^{-1} \\ &\cdot \left(\mathbf{I}_2 - \mathbf{P}_{12}(h_+, h_-) \cdot \mathbf{P}_{22}^{-1}(h_+, h_-) \cdot \mathbf{W}^{+-1}\right)\end{aligned}$$

or

$$\begin{aligned}\mathbf{r} &= -\left(\mathbf{I}_2 + \mathbf{P}_{12}(h_+, h_-) \cdot \left(\mathbf{W}^+ \cdot \mathbf{P}_{22}(h_+, h_-)\right)^{-1}\right)^{-1} \\ &\quad \cdot \left(\mathbf{I}_2 - \mathbf{P}_{12}(h_+, h_-) \cdot \left(\mathbf{W}^+ \cdot \mathbf{P}_{22}(h_+, h_-)\right)^{-1}\right) \\ &= \left(\mathbf{P}_{12}(h_+, h_-) - \mathbf{W}^+ \cdot \mathbf{P}_{22}(h_+, h_-)\right) \\ &\quad \cdot \left(\mathbf{P}_{12}(h_+, h_-) + \mathbf{W}^+ \cdot \mathbf{P}_{22}(h_+, h_-)\right)^{-1}\end{aligned} \tag{14}$$

which is in agreement with [9, p. 11].

5.3. Uniaxial Materials

The theorem in Section 3.4 shows that the inhomogeneous transition region in general is anisotropic. A special case of anisotropy with many applications is the uniaxial case. In this section we treat the propagators for such a material in some detail. In [16] the propagators for homogeneous uniaxial materials are derived for some special cases, and in this section we extend these results to inhomogeneous profiles. The material is assumed to be non-magnetic, $\mu_+ = \mu_- = 1$.

The permittivity dyadic of the uniaxial medium can be written as

$$\boldsymbol{\epsilon}(x_3) = \epsilon_\perp(x_3)\,(\mathbf{I}_3 - \hat{\boldsymbol{u}}\hat{\boldsymbol{u}}) + \epsilon_\parallel(x_3)\hat{\boldsymbol{u}}\hat{\boldsymbol{u}}$$

where the unit normal vector $\hat{\boldsymbol{u}}$ defines the optical axis of the material. The permittivity $\epsilon_\parallel(x_3)$ is the permittivity along the optical axis and $\epsilon_\perp(x_3)$ is the permittivity orthogonal to this direction.

To proceed, the Maxwell equations are rewritten in a system of first order equations in the tangential components [16]

$$\begin{aligned}\frac{\mathrm{d}}{\mathrm{d}x_3}\begin{pmatrix}\boldsymbol{E}_t(x_3)\\ \eta_0\mathbf{J}\cdot\boldsymbol{H}_t(x_3)\end{pmatrix} &= \mathrm{i}k_0\mathbf{M}(\boldsymbol{k}_t,x_3)\cdot\begin{pmatrix}\boldsymbol{E}_t(x_3)\\ \eta_0\mathbf{J}\cdot\boldsymbol{H}_t(x_3)\end{pmatrix}\\ &= \mathrm{i}k_0\begin{pmatrix}\mathbf{M}_{11}(\boldsymbol{k}_t,x_3) & \mathbf{M}_{12}(\boldsymbol{k}_t,x_3)\\ \mathbf{M}_{21}(\boldsymbol{k}_t,x_3) & \mathbf{M}_{22}(\boldsymbol{k}_t,x_3)\end{pmatrix}\cdot\begin{pmatrix}\boldsymbol{E}_t(x_3)\\ \eta_0\mathbf{J}\cdot\boldsymbol{H}_t(x_3)\end{pmatrix}\end{aligned}$$

The blocks of the material dyadic, $\mathbf{M}_{ij}(\boldsymbol{k}_t,x_3)$, $i,j=1,2$, for a nonmagnetic, electrically uniaxial material are [16]

$$\begin{cases}\mathbf{M}_{11} = -\dfrac{(\epsilon_\parallel(x_3)-\epsilon_\perp(x_3))u_3}{k_0\left(\epsilon_\perp+(\epsilon_\parallel-\epsilon_\perp)u_3^2\right)}\boldsymbol{k}_t\boldsymbol{u}_t\\ \mathbf{M}_{12} = -\mathbf{I}_2+\dfrac{1}{k_0^2\left(\epsilon_\perp+(\epsilon_\parallel-\epsilon_\perp)u_3^2\right)}\boldsymbol{k}_t\boldsymbol{k}_t\\ \mathbf{M}_{21} = -\epsilon_\perp(x_3)\mathbf{I}_2-\dfrac{\epsilon_\perp(x_3)(\epsilon_\parallel(x_3)-\epsilon_\perp(x_3))}{\epsilon_\perp+(\epsilon_\parallel-\epsilon_\perp)u_3^2}\boldsymbol{u}_t\boldsymbol{u}_t-\dfrac{1}{k_0^2}\mathbf{J}\cdot\boldsymbol{k}_t\boldsymbol{k}_t\cdot\mathbf{J}\\ \mathbf{M}_{22} = -\dfrac{(\epsilon_\parallel(x_3)-\epsilon_\perp(x_3))u_3}{k_0\left(\epsilon_\perp+(\epsilon_\parallel-\epsilon_\perp)u_3^2\right)}\boldsymbol{u}_t\boldsymbol{k}_t=\mathbf{M}_{11}^t\end{cases}\tag{15}$$

where the projection of the unit normal vector $\hat{\boldsymbol{u}}$ on the $\hat{\boldsymbol{e}}_1$-$\hat{\boldsymbol{e}}_2$ plane is $\boldsymbol{u}_t=\mathbf{I}_2\cdot\hat{\boldsymbol{u}}$ and the projection along the $\hat{\boldsymbol{e}}_3$-axis is $u_3=\hat{\boldsymbol{u}}\cdot\hat{\boldsymbol{e}}_3$. The identity dyadic in $\mathbb{R}^2$ is denoted $\mathbf{I}_2$.

Notice that the result holds for materials that are stratified in the $\hat{\boldsymbol{e}}_3$-direction, not only for the homogeneous case.

5.3.1. Vertical Optical Axis

In our first example we let the optical axis be vertical, *i.e.*, $\hat{\boldsymbol{u}}=\hat{\boldsymbol{e}}_3$. We have $\boldsymbol{u}_t=\mathbf{0}$ and the projection along the z-axis is $u_3=1$. The dyadic $\mathbf{M}$ then is, see (15)

$$\begin{cases}\mathbf{M}_{11}(x_3)=\mathbf{M}_{22}(x_3)=\mathbf{0}\\ \mathbf{M}_{12}(x_3) = -(\hat{\boldsymbol{e}}_\parallel\hat{\boldsymbol{e}}_\parallel+\hat{\boldsymbol{e}}_\perp\hat{\boldsymbol{e}}_\perp)+\dfrac{k_t^2}{\epsilon_\parallel(x_3)k_0^2}\hat{\boldsymbol{e}}_\parallel\hat{\boldsymbol{e}}_\parallel\\ \mathbf{M}_{21}(x_3) = -\epsilon_\perp(x_3)(\hat{\boldsymbol{e}}_\parallel\hat{\boldsymbol{e}}_\parallel+\hat{\boldsymbol{e}}_\perp\hat{\boldsymbol{e}}_\perp)+\dfrac{k_t^2}{k_0^2}\hat{\boldsymbol{e}}_\perp\hat{\boldsymbol{e}}_\perp\end{cases}$$

The four two-dimensional propagator dyadics, $\mathbf{P}_{ij}$, $i,j = 1,2$, satisfy the same set of ordinary differential equations (ODE) as the fields [17], *i.e.*,

$$\frac{\mathrm{d}}{\mathrm{d}x_3}\mathbf{P}(\boldsymbol{k}_t, x_3, h_-) = \mathrm{i}k_0\mathbf{M}(\boldsymbol{k}_t, x_3)\cdot\mathbf{P}(\boldsymbol{k}_t, x_3, h_-) \tag{16}$$

together with the initial condition

$$\mathbf{P}(\boldsymbol{k}_t, h_-, h_-) = \begin{pmatrix} \mathbf{P}_{11}(\boldsymbol{k}_t, h_-, h_-) & \mathbf{P}_{12}(\boldsymbol{k}_t, h_-, h_-) \\ \mathbf{P}_{21}(\boldsymbol{k}_t, h_-, h_-) & \mathbf{P}_{22}(\boldsymbol{k}_t, h_-, h_-) \end{pmatrix} = \begin{pmatrix} \mathbf{I}_2 & \mathbf{0} \\ \mathbf{0} & \mathbf{I}_2 \end{pmatrix} = \mathbf{I}_4$$

Due to the fact that $\mathbf{M}_{11} = \mathbf{M}_{22} = \mathbf{0}$, we immediately see that propagator equation, (16), splits into two non-coupling sets, *viz.*,

$$\begin{cases} \dfrac{\mathrm{d}}{\mathrm{d}x_3}\mathbf{P}_{11}(x_3, h_-) = \mathrm{i}k_0\mathbf{M}_{12}(x_3)\cdot\mathbf{P}_{21}(x_3, h_-) \\ \dfrac{\mathrm{d}}{\mathrm{d}x_3}\mathbf{P}_{21}(x_3, h_-) = \mathrm{i}k_0\mathbf{M}_{21}(x_3)\cdot\mathbf{P}_{11}(x_3, h_-) \end{cases}$$

and

$$\begin{cases} \dfrac{\mathrm{d}}{\mathrm{d}z}\mathbf{P}_{12}(x_3, h_-) = \mathrm{i}k_0\mathbf{M}_{12}(x_3)\cdot\mathbf{P}_{22}(x_3, h_-) \\ \dfrac{\mathrm{d}}{\mathrm{d}z}\mathbf{P}_{22}(x_3, h_-) = \mathrm{i}k_0\mathbf{M}_{21}(x_3)\cdot\mathbf{P}_{12}(x_3, h_-) \end{cases}$$

which is a relation between two of the propagators $\mathbf{P}_{ij}(x_3, h_-)$.

The propagators are diagonal in the basis $\{\hat{\boldsymbol{e}}_\parallel, \hat{\boldsymbol{e}}_\perp\}$, *i.e.*,

$$\mathbf{P}_{ij}(x_3, h_-) = P_{ij}^{\mathrm{TM}}(x_3, h_-)\hat{\boldsymbol{e}}_\parallel\hat{\boldsymbol{e}}_\parallel + P_{ij}^{\mathrm{TE}}(x_3, h_-)\hat{\boldsymbol{e}}_\perp\hat{\boldsymbol{e}}_\perp, \quad i,j = 1,2$$

The TM-case, $\parallel$-polarization, splits in two non-coupling sets of first order ordinary differential equations.

$$\begin{cases} \dfrac{\mathrm{d}}{\mathrm{d}x_3}P_{11}^{\mathrm{TM}} = \mathrm{i}k_0\left(\dfrac{k_t^2}{k_0^2\epsilon_\parallel(x_3)} - 1\right)P_{21}^{\mathrm{TM}} \\ \dfrac{\mathrm{d}}{\mathrm{d}x_3}P_{21}^{\mathrm{TM}} = -\mathrm{i}k_0\epsilon_\perp(x_3)P_{11}^{\mathrm{TM}} \end{cases} \qquad \begin{cases} P_{11}^{\mathrm{TM}}(h_-, h_-) = 1 \\ P_{21}^{\mathrm{TM}}(h_-, h_-) = 0 \end{cases}$$

$$\begin{cases} \dfrac{\mathrm{d}}{\mathrm{d}x_3}P_{12}^{\mathrm{TM}} = \mathrm{i}k_0\left(\dfrac{k_t^2}{k_0^2\epsilon_\parallel(x_3)} - 1\right)P_{22}^{\mathrm{TM}} \\ \dfrac{\mathrm{d}}{\mathrm{d}x_3}P_{22}^{\mathrm{TM}} = -\mathrm{i}k_0\epsilon_\perp(x_3)P_{12}^{\mathrm{TM}} \end{cases} \qquad \begin{cases} P_{12}^{\mathrm{TM}}(h_-, h_-) = 0 \\ P_{22}^{\mathrm{TM}}(h_-, h_-) = 1 \end{cases} \tag{17}$$

Note that the equations are similar, but the initial conditions differ.

For the other polarization, $\perp$-polarization, we obtain the TE-case, which also splits in two non-coupling sets of first order ordinary differential equations.

$$\begin{cases} \dfrac{\mathrm{d}}{\mathrm{d}x_3} P_{11}^{\mathrm{TE}} = -\mathrm{i}k_0 P_{21}^{\mathrm{TE}} \\ \dfrac{\mathrm{d}}{\mathrm{d}x_3} P_{21}^{\mathrm{TE}} = \mathrm{i}k_0 \left(\dfrac{k_t^2}{k_0^2} - \epsilon_\perp(x_3) \right) P_{11}^{\mathrm{TE}} \end{cases} \qquad \begin{cases} P_{11}^{\mathrm{TE}}(h_-, h_-) = 1 \\ P_{21}^{\mathrm{TE}}(h_-, h_-) = 0 \end{cases}$$

$$\begin{cases} \dfrac{\mathrm{d}}{\mathrm{d}x_3} P_{12}^{\mathrm{TE}} = -\mathrm{i}k_0 P_{22}^{\mathrm{TE}} \\ \dfrac{\mathrm{d}}{\mathrm{d}x_3} P_{22}^{\mathrm{TE}} = \mathrm{i}k_0 \left(\dfrac{k_t^2}{k_0^2} - \epsilon_\perp(x_3) \right) P_{12}^{\mathrm{TE}} \end{cases} \qquad \begin{cases} P_{12}^{\mathrm{TE}}(h_-, h_-) = 0 \\ P_{22}^{\mathrm{TE}}(h_-, h_-) = 1 \end{cases} \tag{18}$$

Again, the equations are similar, but the initial conditions differ.

For a general permittivity profile, the equations (17) an (18) have to be solved numerically.

5.3.2. Homogeneous Case

For an homogeneous profile the propagator dyadics can be found explicitly. The general solution of (16) for an homogeneous profile is ($\mathbf{M}$ independent of x_3). The result is

$$\mathbf{P}(\boldsymbol{k}_t, x_3, h_-) = \mathrm{e}^{\mathrm{i}k_0(x_3 - h_-)\mathbf{M}(\boldsymbol{k}_t)}$$

where the material dyadic $\mathbf{M}$ has the form

$$\mathbf{M} = \begin{pmatrix} \mathbf{0} & \mathbf{M}_{12} \\ \mathbf{M}_{21} & \mathbf{0} \end{pmatrix}$$

This form of dyadic has four distinct eigenvalues, *viz.*,

$$\lambda_{1,2,3,4} = \pm\sqrt{\frac{1}{2}\mathrm{Tr}\,(\mathbf{M}_{12}\cdot\mathbf{M}_{21}) \pm \sqrt{\frac{1}{4}\left(\mathrm{Tr}\,(\mathbf{M}_{12}\cdot\mathbf{M}_{21})\right)^2 - \det\,(\mathbf{M}_{12}\cdot\mathbf{M}_{21})}}$$

which are arranged in two pairs ($\lambda_+^2 \neq \lambda_-^2$)

$$\lambda_1 = -\lambda_4 = \lambda_+, \qquad \lambda_2 = -\lambda_3 = \lambda_-$$

The propagator can then be obtained as [16] ($d = x_3 - h_-$)

$$\begin{aligned} e^{ik_0 d\mathbf{M}} =& \frac{1}{\lambda_-^2 - \lambda_+^2} \left(\mathbf{I}_4 \lambda_-^2 - \mathbf{M}\cdot\mathbf{M}\right) \\ & \cdot \left(\mathbf{I}_4 \cos\left(k_0 d\lambda_+\right) + \frac{i}{\lambda_+}\mathbf{M}\sin\left(k_0 d\lambda_+\right)\right) \\ & - \frac{1}{\lambda_-^2 - \lambda_+^2} \left(\mathbf{I}_4 \lambda_+^2 - \mathbf{M}\cdot\mathbf{M}\right) \\ & \cdot \left(\mathbf{I}_4 \cos\left(k_0 d\lambda_-\right) + \frac{i}{\lambda_-}\mathbf{M}\sin\left(k_0 d\lambda_-\right)\right) \end{aligned}$$

5.3.3. One-Dimensional Profile

For a one-dimensional profile the homogenized permittivity profile is given by (9). Moreover, in this case the optical axis is $\hat{\boldsymbol{u}} = \hat{\boldsymbol{e}}_1$ and therefore $u_3 = 0$, which imply that the dyadic $\mathbf{M}$ is, see (15)

$$\begin{cases} \mathbf{M}_{11} = \mathbf{M}_{22} = \mathbf{0} \\ \mathbf{M}_{12} = -\mathbf{I}_2 + \frac{k_t^2}{\langle\epsilon\rangle(x_3)k_0^2}\hat{\boldsymbol{e}}_\parallel\hat{\boldsymbol{e}}_\parallel \\ \mathbf{M}_{21} = -\frac{\hat{\boldsymbol{e}}_1\hat{\boldsymbol{e}}_1}{\langle 1/\epsilon\rangle(x_3)} - \langle\epsilon\rangle(x_3)\hat{\boldsymbol{e}}_2\hat{\boldsymbol{e}}_2 + \frac{k_t^2}{k_0^2}\hat{\boldsymbol{e}}_\perp\hat{\boldsymbol{e}}_\perp \end{cases}$$

since by (9) $\epsilon_\parallel^{-1}(x_3) = \langle 1/\epsilon\rangle(x_3)$ and $\epsilon_\perp(x_3) = \langle\epsilon\rangle(x_3)$. The results in Section 5.3.2 can then be applied to obtain the propagators.

6. EXAMPLES

In this section, we present two examples that illustrate the theory developed in this paper. In the first example the corrugations have a circular cross section so the material is uniaxial with optical axis $\hat{\boldsymbol{u}} = \hat{\boldsymbol{e}}_3$. The second is the most simple one-dimension case with constant-width corrugations. This second case can be solved analytically by the results in Sections 5.3.3 and 5.3.2.

6.1. Conical Corrugations

Consider circular cones with radius at the base b and height h in a quadratic lattice with periodicity a, see Figure 4. This geometry has important applications in radar absorbing materials and has been treated in the literature with different methods [4, 5, 10]. The permittivity of the inclusion is ϵ_-. These cones are on top of an

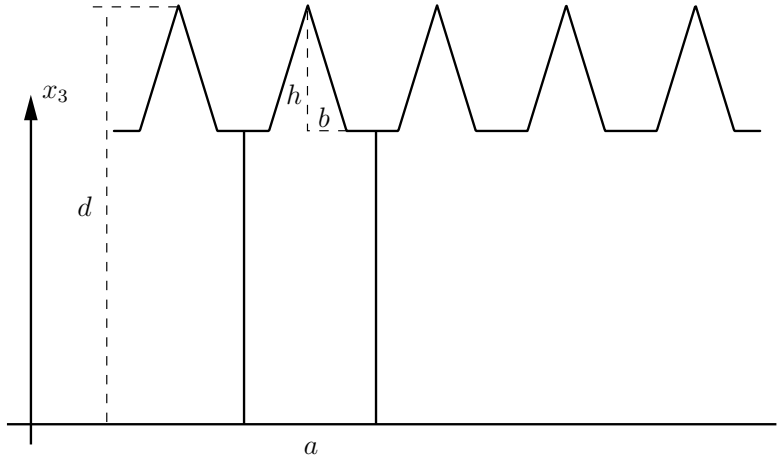

Figure 4. The geometry of the cones in Section 6.1.

isotropic material with the same permittivity ϵ_- such that the total height is d. The radius $r(x_3)$ of the cones then varies in the interval $]d-h, d[$ as

$$r(x_3) = b\,(d - x_3)\,/h, \quad (d-h) < x_3 \leq d$$

The cone structure is backed with a perfectly conducting plane at $x_3 = 0$.

The Maxwell Garnett mixture formula [19] is used as an approximation to the solution of the local problem, (8), in two spatial dimensions. Due to the circular symmetry of the problem this approximation is very good [7]. We get

$$\epsilon_{\text{eff}} = 1 + \frac{2f(\epsilon_{\text{r}} - 1)}{2 + (1-f)(\epsilon_{\text{r}} - 1)}$$

The permittivity ϵ_{r} is relative to the background permittivity ϵ_+, *i.e.*, $\epsilon_{\text{r}} = \epsilon_-/\epsilon_+$, and f is the volume fraction of the inclusion.

The homogenized material becomes uniaxial with vertical optical axis, and by the Theorem in Section 3.4, we get

$$\begin{cases} \epsilon_{\parallel}(x_3) = \begin{cases} \epsilon_-, & 0 \leq x_3 \leq (d-h) \\ \epsilon_+ + (\epsilon_- - \epsilon_+)\dfrac{\pi r^2(x_3)}{a^2}, & (d-h) < x_3 \leq d \end{cases} \\ \epsilon_{\perp}(x_3) = \begin{cases} \epsilon_-, & 0 \leq x_3 \leq (d-h) \\ \epsilon_+ + \dfrac{2\pi r^2(x_3)(\epsilon_- - \epsilon_+)/a^2}{2\epsilon_+ + (1 - \pi r^2(x_3)/a^2)(\epsilon_- - \epsilon_+)}, & (d-h) < x_3 \leq d \end{cases} \end{cases}$$

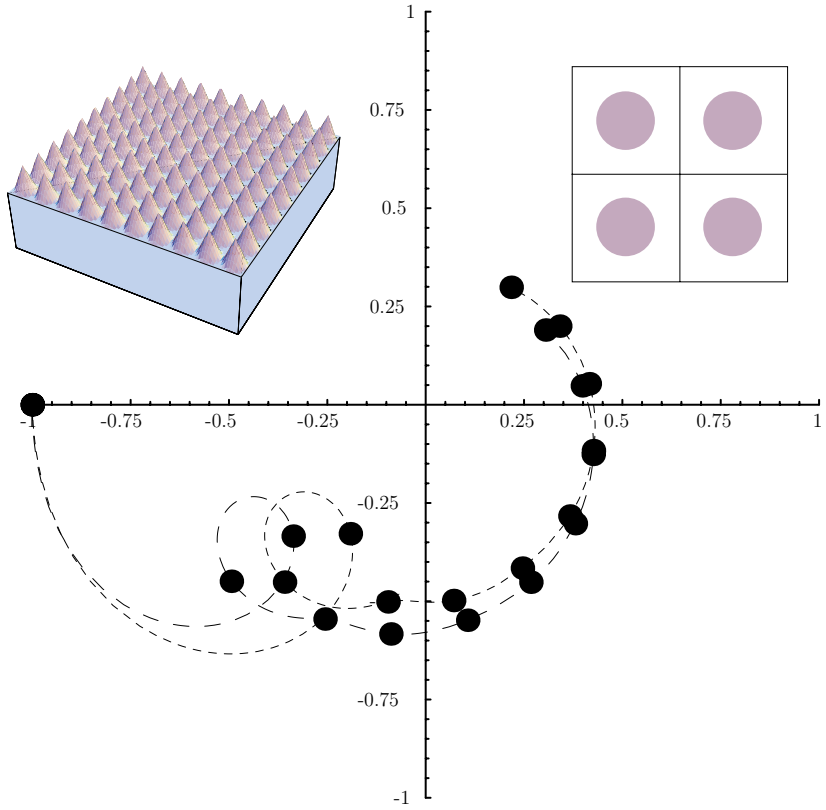

Figure 5. The reflection dyadic in the complex plane for the cone geometry shown in the inserted figure. The cone structure is backed with a perfectly conducting plane. The material parameters are $b/a = 0.45$, $h/d = 0.3$, $d/a = 6$, $\theta = 30°$, $\epsilon_- = 10(1 + \mathrm{i})$, and $\epsilon_+ = 1$. The finer dashed line depicts the TM-case and the coarser dashed line the TE-mode. The frequency varies along the curve. The dots show $k_0 a = 0, 0.1, 0.2, \ldots, 1$ ($k_0 a = 0$ at -1).

These values of the permittivity are then used in the numerical solution of equations (17) and (18) to find the propagators. The reflection dyadics is then found by utilizing the results in Section 5.2. The result is depicted in Figure 5. For high frequencies the homogenized profile does not model the interaction of the incident electromagnetic wave with the cone structure very adequately, but independent computations indicate that the solution is accurate up to $k_0 a \approx 0.2$–0.3 [20].

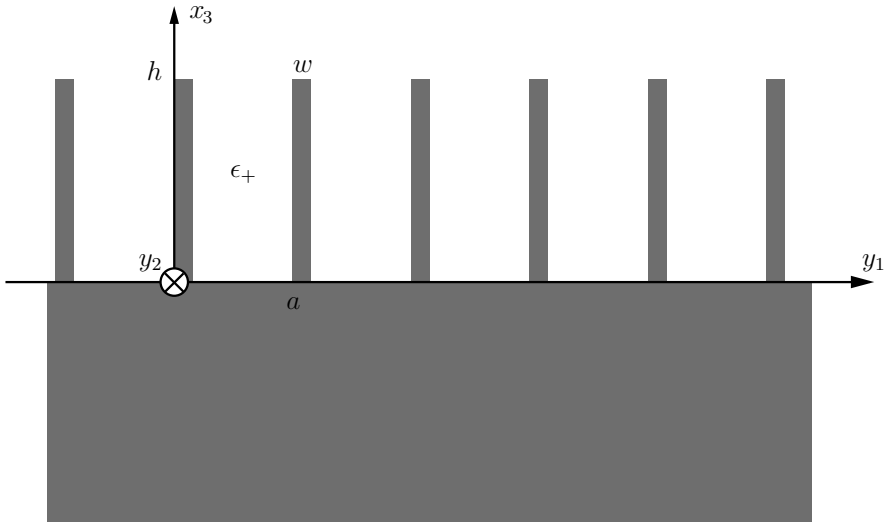

Figure 6. The geometry of the problem in Section 6.2.

6.2. One-Dimensional Example

The most simple one-dimensional geometry is depicted in Figure 6. The width of the corrugations in this case is constant and the transition layer is therefore homogeneous.

In the limit of a perfectly conducting material in the lower medium, we get in the $\hat{\boldsymbol{e}}_1$-$\hat{\boldsymbol{e}}_2$-basis

$$\mathbf{Z} = \begin{pmatrix} -\mathrm{i}\dfrac{\tan(k_0 h\Psi)}{\Psi} & 0 \\ 0 & 0 \end{pmatrix}$$

where $\Psi = \sqrt{\epsilon_{11} - \sin^2\theta\sin^2\phi} = \sqrt{\epsilon_{11} - k_y^2/k_0^2}$, and $\epsilon_{11} = \epsilon_+ a/(a-w)$ ($0 < w < a$ is the width of the ridges, h is their heights, and a is the periodicity of the corrugations, see Figure 6). This result is consistent with the result reported in [6] provided the permittivity of the material in the trough is interpreted as ϵ_{11}.

The reflection dyadics of the corrugated surface is

$$\mathbf{r} = \begin{pmatrix} -\dfrac{\Psi\cos\theta + \mathrm{i}\big(1-\sin^2\theta\sin^2\phi\big)\tan(k_0 h\Psi)}{\Psi\cos\theta - \mathrm{i}\big(1-\sin^2\theta\sin^2\phi\big)\tan(k_0 h\Psi)} & \dfrac{-2\mathrm{i}\sin^2\theta\sin\phi\cos\phi\tan(k_0 h\Psi)}{\Psi\cos\theta - \mathrm{i}\big(1-\sin^2\theta\sin^2\phi\big)\tan(k_0 h\Psi)} \\ 0 & -1 \end{pmatrix}$$

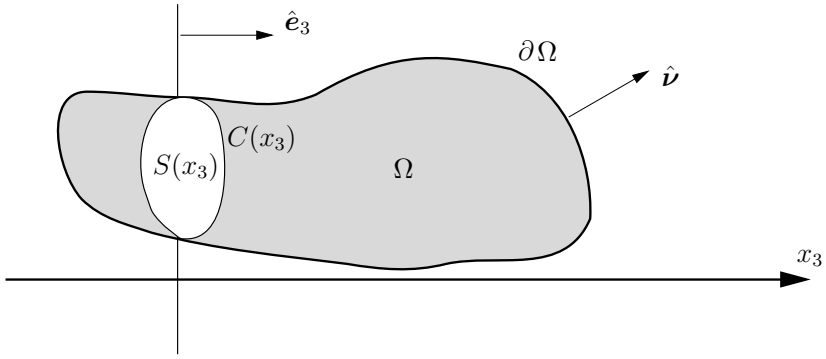

Figure A1. The cross section area $S(x_3)$ of the intersection between Ω and the plane $x_3 =$ constant. The plane $S(x_3)$ is perpendicular to the $\hat{\boldsymbol{e}}_3$-axis.

7. CONCLUSIONS

It is shown in this paper that a corrugated surface can be replaced by an inhomogeneous transition region in the limit of vanishing periodicity of the corrugations. The explicit expressions of the homogenized permittivity and permeability profiles can be obtained by solving a two-dimensional local problem. Several cases can be solved analytically, which leads to simple numerical computations.

ACKNOWLEDGMENT

The work reported in this paper is supported by a grant from the Swedish Foundation for Strategic Research (SSF), which is gratefully acknowledged.

APPENDIX A. DIFFERENTIAL GEOMETRY

Lemma A.1. *Assume Ω is a bounded, open set in $\mathbb{R}^3$ with $C^{1,1}$ boundary, $\partial\Omega$. The outward pointing unit normal vector to $\partial\Omega$ is $\hat{\boldsymbol{\nu}}$, see Figure A1. We denote by $S(x_3)$ the intersection between Ω and the plane $x_3 =$ constant. The boundary curve of $S(x_3)$ is denoted $C(x_3)$, and the outward pointing unit normal vector to this curve in the plane $x_3 =$ constant is denoted $\hat{\boldsymbol{n}}$. Then, for every function $f \in H^1(\Omega)$, we*

have

$$\iint\limits_{S(x_3)} \frac{\partial f(\boldsymbol{\rho},x_3)}{\partial x_3}\,\mathrm{d}S_{\boldsymbol{\rho}} = F'(x_3) + \int\limits_{C(x_3)} f(\boldsymbol{\rho},x_3)\frac{\hat{\boldsymbol{\nu}}\cdot\hat{\boldsymbol{e}}_3}{\hat{\boldsymbol{\nu}}\cdot\hat{\boldsymbol{n}}}\,\mathrm{d}l_{\boldsymbol{\rho}}$$

where the position vector in the $\hat{\boldsymbol{e}}_1$-$\hat{\boldsymbol{e}}_2$*-plane is denoted* $\boldsymbol{\rho} = \hat{\boldsymbol{e}}_1 x_1 + \hat{\boldsymbol{e}}_2 x_2$*, and*

$$F(x_3) = \iint\limits_{S(x_3)} f(\boldsymbol{\rho},x_3)\,\mathrm{d}S_{\boldsymbol{\rho}}$$

Here $\mathrm{d}S_{\boldsymbol{\rho}} = \mathrm{d}x_1\mathrm{d}x_2$ *denotes the surface measure of* $S(x_3)$*, and* $\mathrm{d}l_{\boldsymbol{\rho}}$ *denotes the curve measure of* $C(x_3)$*, which is oriented such that the direction in the right-hand sense coincides with the positive* $\hat{\boldsymbol{e}}_3$*-direction.*

Proof of Lemma A.1: Let $\eta > 0$ and apply the divergence theorem to a vector-valued field $\hat{\boldsymbol{e}}_3 f(\boldsymbol{\rho},x_3)$ in the volume V, which is a subset of Ω bounded between $S(x_3)$ and $S(x_3+\eta)$. The result is

$$\iiint\limits_{V} \nabla\cdot\left(\hat{\boldsymbol{e}}_3 f(\boldsymbol{\rho},x_3)\right)\,\mathrm{d}v = F(x_3+\eta) - F(x_3) + \iint\limits_{\partial\Omega\cap\overline{V}} \left(\hat{\boldsymbol{\nu}}\cdot\hat{\boldsymbol{e}}_3\right) f(\boldsymbol{\rho},x_3)\,\mathrm{d}S$$

where $\mathrm{d}v$ denotes the volume measure of Ω , and $\mathrm{d}S$ denotes the surface measure of $\partial\Omega$. In the limit $\eta \to 0$ we get

$$\iint\limits_{S(x_3)} \frac{\partial f(\boldsymbol{\rho},x_3)}{\partial x_3}\,\mathrm{d}S_{\boldsymbol{\rho}} = F'(x_3) + \int\limits_{C(x_3)} f(\boldsymbol{\rho},x_3)\frac{\hat{\boldsymbol{\nu}}\cdot\hat{\boldsymbol{e}}_3}{\hat{\boldsymbol{\nu}}\cdot\hat{\boldsymbol{n}}}\,\mathrm{d}l_{\boldsymbol{\rho}}$$

since for sufficiently small η, $\mathrm{d}v = \eta\mathrm{d}S_{\boldsymbol{\rho}}$, and $\mathrm{d}S = \eta\mathrm{d}l_{\boldsymbol{\rho}}/(\hat{\boldsymbol{\nu}}\cdot\hat{\boldsymbol{n}})$, and the lemma is proven.

Corollary A.1. *If the surface* $\partial\Omega$ *be defined by* $x_3 = h(\boldsymbol{\rho})$*, then*

$$\frac{\hat{\boldsymbol{\nu}}\cdot\hat{\boldsymbol{e}}_3}{\hat{\boldsymbol{\nu}}\cdot\hat{\boldsymbol{n}}} = \frac{\pm 1}{|\nabla_{\boldsymbol{y}} h(\boldsymbol{y})|}$$

The plus-sign is applicable if $\hat{\boldsymbol{n}}\cdot\nabla_{\boldsymbol{y}} h < 0$ *and the minus-sign if* $\hat{\boldsymbol{n}}\cdot\nabla_{\boldsymbol{y}} h > 0$*. The Lemma A becomes*

$$\iint\limits_{S(x_3)} \frac{\partial f(\boldsymbol{\rho},x_3)}{\partial x_3}\,\mathrm{d}S_{\boldsymbol{\rho}} = F'(x_3) \pm \int\limits_{C(x_3)} \frac{f(\boldsymbol{\rho},x_3)}{|\nabla_{\boldsymbol{y}} h(\boldsymbol{y})|}\,\mathrm{d}l_{\boldsymbol{\rho}}$$

Proof of Corollary A.1: This is easily proven by using the form of the normal vectors $\hat{\boldsymbol{\nu}}$ and $\hat{\boldsymbol{n}}$ in Section 2.

REFERENCES

1. Bensoussan, A., J. L. Lions, and G. Papanicolaou, *Asymptotic Analysis for Periodic Structures*, Vol. 5 of *Studies in Mathematics and its Applications*, North-Holland, Amsterdam, 1978.
2. Felbacq, D., "Comments on "Photonic band gaps: Noncommuting limit and the 'acoustic band'"," arXiv:cond-mat/0104488 v1, April 25, 2001.
3. Holloway, C. L. and E. F. Kuester, "Effective boundary conditions for rough surfaces with a thin cover," *Antennas and Propagation Society, IEEE International Symposium 1999*, Vol. 1, 506–509, 1999.
4. Holloway, C. L. and E. F. Kuester, "A low-frequency model for wedge or pyramid absorber arrays—II: Computed and measured results," *IEEE Trans. Electromagn. Compatibility*, Vol. 36, No. 4, 307–313, 1994.
5. Janaswamy, R., "Oblique scattering from lossy periodic surfaces with application to anechoic chamber absorbers," *IEEE Trans. Antennas Propagat.*, Vol. 40, No. 2, 162–169, 1992.
6. Kildal, P. S., "Artificially soft and hard surfaces in electromagnetics," *IEEE Trans. Antennas Propagat.*, Vol. 38, No. 10, 1537–1544, 1990.
7. Kristensson, G., "Homogenization of spherical inclusions," *Progress In Electromagnetics Research*, J. A. Kong (ed.), PIER 42, 1–25, EMW Publishing, Cambridge, MA, 2003.
8. Kristensson, G., S. Poulsen, and S. Rikte, "Propagators and scattering of electromagnetic waves in planar bianisotropic slabs — an application to frequency selective structures," *Progress In Electromagnetics Research*, J. A. Kong (ed.), PIER 48, 1–25, EMW Publishing, Cambridge, MA, 2004.
9. Kristensson, G., P. Waller, and A. Derneryd, "Radiation efficiency and surface waves for patch antennas on inhomogeneous substrates," *IEE Proc. — Microw. Antennas Propag.*, Vol. 150, No. 6, 477–483, December 2003.
10. Kuester, E. F. and C. L. Holloway, "A low-frequency model for wedge or pyramid absorber arrays—I: Theory," *IEEE Trans. Electromagn. Compatibility*, Vol. 36, No. 4, 300–306, 1994.
11. McPhedran, R. C., N. A. Nicorovici, and L. C. Botten, "The

TEM mode and homogenization of doubly periodic structures," *J. Electro. Waves Applic.*, Vol. 11, No. 7, 981–1012, 1997.

12. Milton, G. W., *The Theory of Composites*, Cambridge University Press, Cambridge, U.K., 2002.
13. Nevard, J. and J. B. Keller, "Homogenization of rough boundaries and interfaces," *SIAM J. Appl. Math.*, Vol. 57, No. 6, 1660–1686, 1997.
14. Nicorovici, N. A., R. C. McPhedran, and L. C. Botten, "Photonic band gaps for arrays of perfectly conducting cylinders," *Phys. Rev. E*, Vol. E52, No. 1, 1135–1145, 1995.
15. Nicorovici, N. A., R. C. McPhedran, and L. C. Botten, "Photonic band gaps: Noncommuting limits and the 'acoustic band'," *Phys. Rev. Lett.*, Vol. 75, No. 8, 1507–1510, 1995.
16. Rikte, S., G. Kristensson, and M. Andersson, "Propagation in bianisotropic media—reflection and transmission," Technical Report LUTEDX/(TEAT-7067)/1–31/(1998), Lund Institute of Technology, Department of Electromagnetic Theory, P.O. Box 118, S-221 00 Lund, Sweden, 1998.
17. Rikte, S., G. Kristensson, and M. Andersson, "Propagation in bianisotropic media—reflection and transmission," *IEE Proc. Microwaves, Antennas and Propagation*, Vol. 148, No. 1, 29–36, 2001.
18. Sanchez-Palencia, E., *Non-Homogeneous media and Vibration Theory*, No. 127 in Lecture Notes in Physics, Springer-Verlag, Berlin, 1980.
19. Sihvola, A., *Electromagnetic Mixing Formulae and Applications*, IEE Electromagnetic Waves Series, 47, Institution of Electrical Engineers, 1999.
20. Sjöberg, D., C. Engström, G. Kristensson, D. J. N. Wall, and N. Wellander, "A Floquet-Bloch decomposition of Maxwell's equations, applied to homogenization," Technical Report LUTEDX/(TEAT-7119)/1–28/(2003), Lund Institute of Technology, Department of Electroscience, P.O. Box 118, S-221 00 Lund, Sweden, 2003. `http://www.es.lth.se`.

Gerhard Kristensson received his B.S. degree in mathematics and physics in 1973, and the Ph.D. degree in theoretical physics in 1979, both from the University of Göteborg, Sweden. In 1983 he was appointed Docent in theoretical physics at the University of Göteborg. He has held positions at the University of Göteborg and the Royal Institute of Technology in Stockholm before being appointed Chair of

Electromagnetic Theory at Lund Institute of Technology. He has held visiting positions at Ames Laboratory (Iowa State University) and at the University of Canterbury (New Zealand). Currently, Kristensson is a member of the Advisory Board for *Inverse Problems*, the Board of Editors of *Wave Motion*, and the Editorial and Review Board for *Journal of Electromagnetic Waves and Applications* and *Progress in Electromagnetic Research*. He is the Official Member of URSI, Commission B for Sweden and a Fellow of the Institute of Physics, England. Kristensson's major research interests are focused on wave propagation in inhomogeneous media, including inverse scattering problems and dispersion effects in anisotropic and bi-anisotropic media. Antennas, especially antennas in mobile communications, are also of interest, as well as radome design problems, frequency selective structures, and homogenization of complex materials.